Chapter 6

Stability and nonlinear dynamics in thyristor and diode circuits

preprint March 22 2001
chapter 6 in Nonlinear Phenomena in Power Electronics:
Attractors, Bifurcations, Chaos, and Nonlinear Control
Editors S. Banerjee, G.C. Verghese,
IEEE Press, to appear in Spring 2001

Ian Dobson
Electrical and Computer Engineering Department
University of Wisconsin-Madison USA
1415 Engineering Drive
Madison WI 53706 USA
phone (608) 262 2661
fax (608) 262 1267
dobson@engr.wisc.edu

Contents

6 Stability and nonlinear dynamics in thyristor and diode circuits 1
6.1 Introduction . . . 2
6.2 Ideal diode and thyristor switching rules . . . 3
6.3 Static VAR system example . . . 4
6.4 Poincaré map . . . 6
6.5 Jacobian of Poincaré map . . . 8
6.5.1 Thyristor current function and transversality . . . 9
6.5.2 Relations between on and off systems . . . 10
6.5.3 Derivation of Jacobian formula . . . 11
6.5.4 Discussion of Jacobian formula . . . 14
6.6 Switching damping . . . 15
6.6.1 Simple example . . . 15
6.6.2 Switching damping in the SVC example . . . 17
6.6.3 Variational equation . . . 17
6.7 Switching time bifurcations . . . 20
6.7.1 Switching time bifurcations and instability . . . 20
6.7.2 Switching time bifurcations for transients . . . 23
6.7.3 Misfire onset as a transcritical bifurcation . . . 24
6.7.4 Noninvertibility and discontinuity of the Poincaré map . . . 27
6.7.5 Multiple attractors and their basin boundaries . . . 28
6.8 Diode circuits . . . 30
6.8.1 Transversality and Poincaré map Jacobian formula . . . 30
6.8.2 Poincaré map Jacobian for the DC-DC buck-boost convertor in discontinuous mode . . . 31
6.8.3 Poincaré map continuity and switching time bifurcations . . . 32
6.9 Firing angle control . . . 33

6.1 Introduction

This chapter explains aspects of stability, bifurcation and nonlinear dynamics in ideal thyristor and diode circuits. Thyristor circuits exhibit many interesting and unusual dynamical features and are of technological importance at high power levels up to MW utility power levels. Highlights of the chapter include useful simplifications in

computing stability, the damping inherent in thyristor turn off, jumps or bifurcations in switching times and repeated violation of the behavior normally expected in smooth nonlinear dynamical systems. Thyristors and diodes constrain their currents to zero when they are off. This important constraint is accounted for by changing the state space dimension as thyristors or diodes switch on and off. The inhibition of thyristor turn on until a firing pulse is present has a significant effect on the system dynamics.

The ideas are mainly developed for the regularly fired thyristor circuit for static VAR control introduced in Chapter 2 but almost all results can be generalized. The chapter also outlines the modifications required for diode circuits and for thyristor circuits with feedback control of the firing times. The chapter is mainly based on work by Dobson, Jalali, Rajaraman and Lasseter [4, 5, 14, 13, 15, 24, 25], which, in turn, builds on work by von Lutz, Grötzbach, Chua, Hasler and Verghese [17, 6, 1, 30] and the pioneering work of Louis [11]. Most of the chapter material first appeared in conferences [12, 3, 23]. Wolf et al. [31] present an alternative account of switching time bifurcations and their effect on the Poincaré map.

We briefly indicate some applications of the ideas and calculations in this chapter. The Poincaré map Jacobian can be used with Newton-Raphson methods to compute periodic orbits of power electronic circuits [6]. Resonances are predicted in an SVC circuit in [4] and more generally in [24]. The dynamics of the thyristor controlled series capacitor are studied in [13, 22, 20]. The effects of the thyristor controlled series capacitor on subsynchronous resonance are studied in [27, 21, 20]. (The exact dynamics of thyristor controlled series capacitor computed in [27] have also been reproduced in [18] using the phasor averaging techniques of Chapter 2.) HVDC dynamics are analyzed in [22].

6.2 Ideal diode and thyristor switching rules

It is useful to idealize the behavior of diodes and thyristors, particularly for high power utility power electronics and for many systems studies at a range of power levels. This section explains the idealized diode and thyristor models used in this chapter.

Ideal diodes and thyristors are either on and modeled as a short circuit or off and modeled as an open circuit. An off diode has a negative voltage; it switches on when the voltage becomes zero. An on diode has a positive current; it switches off when the current becomes zero. Diode switchings are uncontrolled in that they are completely determined by the circuit waveforms.

A thyristor at this level of idealization is a diode that is inhibited from turn on until a firing pulse is present. That is, an on thyristor switches off like a diode and an off thyristor switches on when the voltage is nonnegative and the thyristor firing pulse is on. In particular, if a thyristor receives a firing pulse when its voltage is negative, it does not turn on and the thyristor is said to have "misfired".

Firing pulses are often short (less than 50 μs [10]) and this chapter approximates a short firing pulse by assuming that the firing pulse is on only at one instant of time. Thyristor switch on is controlled by the firing pulse, but the thyristor switch off is determined by the first zero of the thyristor current waveform encountered after switch on.

The dependence of thyristor and diode switching times on the circuit currents and voltages causes significant nonlinearity in thyristor and diode circuits. Moreover, in thyristor circuits the system dynamics are augmented by the rule that the thyristor only switches on when a firing pulse is present. This rule has a major effect on the system dynamics and causes behavior quite different from conventional nonlinear dynamical systems. The novel behavior occurs even in the simplified case in which the firing pulses are periodic and unaffected by the dynamics of the rest of the circuit.

6.3 Static VAR system example

Figure 6.1 shows a single phase static VAR system consisting of a thyristor controlled reactor and a parallel capacitor C. This system is connected to an infinite bus behind a power system impedance of inductance L_s and resistance R_s. The thyristor controlled reactor is modeled as an inductance L_r and resistance R_r in series with back to back thyristors. The source voltage $u(t) = \sin(\omega t - 2\pi/3)$ has frequency $\omega = 2\pi 60$ rad/s and period $T = 2\pi/\omega$. The per unit component values are $L_s = 0.195$ mH, $R_s = 0.9$ mΩ, $L_r = 1.66$ mH, $R_r = 31.3$ mΩ and $C = 1.5$ mF. The SVC modeling is further explained and referenced in [14]. For general background on static VAR compensators see [16, 8, 19].

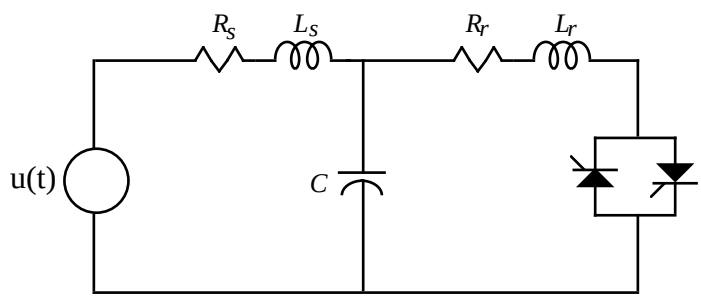

Figure 6.1: Single phase static VAR system.

The switching element of the thyristor controlled reactor consists of two back to back thyristors which conduct on alternate half cycles of the supply frequency. Except in section 6.9, the thyristor firing pulses are assumed to be supplied periodically and the system is controlled by varying the timing delay of the firing pulses. For simplicity, the system is studied in most of the chapter with firing pulse delay as an open loop control parameter. In practice a closed loop control would modify the firing pulse delay.

The idealized operation of a thyristor controlled reactor is explained in Figure 6.2. If the thyristors are fired at the point where the voltage $V_c(t)$ is at a peak, full conduction results. The circuit then operates as if the thyristors were shorted out, resulting in a thyristor current which lags the voltage by nearly 90 degrees. If the firing is delayed past the peak voltage, the thyristor conduction time and the fundamental component of reactive current are reduced.

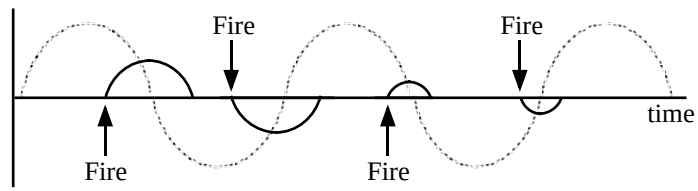

Figure 6.2: Idealized operation of a thyristor controlled reactor (gray line=capacitor voltage V_c, solid line=thyristor current I_r). V_c is also the voltage across the thyristor controlled reactor.

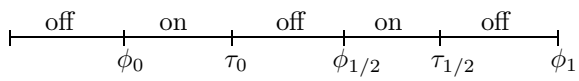

Figure 6.3: Static VAR switchings.

When a thyristor is on, the system state vector $\mathbf{x}(t)$ specifies the thyristor controlled reactor current, capacitor voltage and the source current:

$$\mathbf{x}(t) = \begin{pmatrix} I_r(t) \\ V_c(t) \\ I_s(t) \end{pmatrix} \tag{6.1}$$

and the system dynamics are described by the ON linear system:

$$\dot{\mathbf{x}} = A_{\text{on}}\mathbf{x} + B_{\text{on}}u \tag{6.2}$$

$$\text{where } A_{\text{on}} = \begin{pmatrix} -R_r/L_r & 1/L_r & 0 \\ -1/C & 0 & 1/C \\ 0 & -1/L_s & -R_s/L_s \end{pmatrix} \text{ and } B_{\text{on}} = \begin{pmatrix} 0 \\ 0 \\ 1/L_s \end{pmatrix} \tag{6.3}$$

During the off time of each thyristor, the circuit state is constrained to lie in the plane of zero thyristor current specified by $I_r = 0$. In this mode, the system state vector $\mathbf{y}(t)$ specifies the capacitor voltage and the source current:

$$\mathbf{y}(t) = \begin{pmatrix} V_c(t) \\ I_s(t) \end{pmatrix} \tag{6.4}$$

and the system dynamics are given by the OFF linear system

$$\dot{\mathbf{y}} = A_{\text{off}}\mathbf{y} + B_{\text{off}}u \tag{6.5}$$

$$\text{where } A_{\text{off}} = \begin{pmatrix} 0 & 1/C \\ -1/L_s & -R_s/L_s \end{pmatrix} \text{ and } B_{\text{off}} = \begin{pmatrix} 0 \\ 1/L_s \end{pmatrix} \tag{6.6}$$

Figure 6.3 outlines the system switchings as the system state evolves over a period T. A thyristor starts conducting at time ϕ_0. This mode is described by (6.2)

and ends when the thyristor current goes through zero at time τ_0. The ensuing non-conducting mode is described by (6.5) and continues until the next firing pulse is applied at time $\phi_{1/2}$. This starts a similar on-off cycle which lasts until the next period starts at time $\phi_1 = \phi_0 + T$.

Define R to be the projection matrix

$$R = \begin{pmatrix} 0 & 1 & 0 \\ 0 & 0 & 1 \end{pmatrix} \qquad \text{and} \qquad Q = R^{\mathrm{T}} = \begin{pmatrix} 0 & 0 \\ 1 & 0 \\ 0 & 1 \end{pmatrix} \tag{6.7}$$

(The matrix transpose of R is notated as R^{T}.) The state at the switch on time ϕ_0 is denoted either by the vector $\mathbf{y}(\phi_0)$ or by the vector $\mathbf{x}(\phi_0)$. These representations of the state at the switch on time are related by

$$\mathbf{x}(\phi_0) = Q\mathbf{y}(\phi_0) \qquad \text{or} \qquad \begin{pmatrix} I_r(\phi_0) \\ V_c(\phi_0) \\ I_s(\phi_0) \end{pmatrix} = \begin{pmatrix} 0 & 0 \\ 1 & 0 \\ 0 & 1 \end{pmatrix} \begin{pmatrix} V_c(\phi_0) \\ I_s(\phi_0) \end{pmatrix} \tag{6.8}$$

Equation (6.8) expresses the fact that the $\mathbf{x}$ representation of the state at a switch on is obtained from the $\mathbf{y}$ representation by adding a new first component which has value zero.

The state at the switch off time τ_0 is similarly denoted either by $\mathbf{x}(\tau_0)$ or $\mathbf{y}(\tau_0)$ and these are related by

$$\mathbf{y}(\tau_0) = R\mathbf{x}(\tau_0) \qquad \text{or} \qquad \begin{pmatrix} V_c(\tau_0) \\ I_s(\tau_0) \end{pmatrix} = \begin{pmatrix} 0 & 1 & 0 \\ 0 & 0 & 1 \end{pmatrix} \begin{pmatrix} I_r(\tau_0) \\ V_c(\tau_0) \\ I_s(\tau_0) \end{pmatrix} \tag{6.9}$$

The matrix R in (6.9) may be thought of as projecting the vector $\mathbf{x}$ onto the plane in state space of zero thyristor current.

6.4 Poincaré map

The Poincaré map is a standard tool from dynamical systems theory to study the dynamics of periodic systems [7, 29]. The main idea of this approach is to observe the system states once per cycle and define the Poincaré map as the map which advances the system states by one cycle. If the system state at time t_0 is denoted by $\mathbf{x}(t_0)$, then the Poincaré map P maps the state at time t_0 to the state at time $t_0 + T$:

$$P(\mathbf{x}(t_0)) = \mathbf{x}(t_0 + T) \tag{6.10}$$

(This form of the Poincaré map is called a stroboscopic map in chapter 3; see chapter 3 for other forms of Poincaré map.)

If $\mathbf{x}(t_0)$ is the steady state value of the state $\mathbf{x}$ at time t_0, then $P(\mathbf{x}(t_0)) = \mathbf{x}(t_0 + T) = \mathbf{x}(t_0)$ and the map P has a fixed point at $\mathbf{x}(t_0)$. Fixed points of the Poincaré map P correspond to periodic orbits of the system. If the state $\mathbf{x}(t_0)$ is perturbed from its steady state value, there will be a transient. Samples of this transient once a cycle

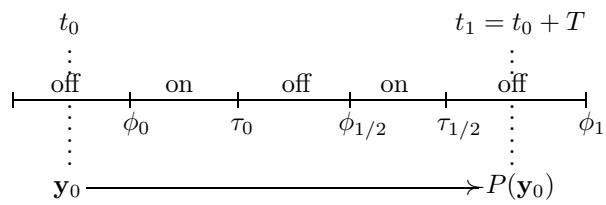

Figure 6.4: Poincaré map P.

can be obtained by applying the Poincaré map successively to the perturbed state $\mathbf{x}(t_0)$. That is, the samples are $\mathbf{x}(t_0)$, $P(\mathbf{x}(t_0))$, $P(P(\mathbf{x}(t_0)))$, $P(P(P(\mathbf{x}(t_0))))$, $\cdots$. The Poincaré map analysis of stability is equivalent to the sampled data approach [30] and Floquet stability theory [9].

One way to visualize the Poincaré map is to suppose that the switching circuit is running in a dark room and a strobe light flashes once every cycle. Suppose that one can observe by measurements the currents and voltages of the system state. Then the Poincaré map is the operation which takes the system state at one flash and constructs the system state at the next flash. If the switching circuit is in a steady state which is a periodic orbit of period one cycle, one will see a fixed point of the Poincaré map. A stable transient will appear as a system state which approaches the steady state at each flash.

Consider the simple example of the linear system

$$\dot{\mathbf{x}} = A\mathbf{x} + Bu \tag{6.11}$$

with state vector $\mathbf{x}$, state matrix A, and input u of period T. The Poincaré map is computed by integrating (6.11) forward for one period T:

$$P(\mathbf{x}(t_0)) = e^{AT}\mathbf{x}(t_0) + \int_{t_0}^{t_0+T} e^{A(t_0+T-s)}Bu(s)ds \tag{6.12}$$

Now we show how to compute the Poincaré map for the SVC circuit example. The Poincaré map P advances the state by one period T. In particular we choose P to advance the state $\mathbf{y}(t_0)$ at time t_0 to $P(\mathbf{y}(t_0)) = \mathbf{y}(t_0 + T)$ as shown in Figure 6.4. P can be computed by integrating the system equations (6.2) and (6.5) and taking into account the coordinate changes (6.8) and (6.9) when the switchings occur [5]. Given a time interval $[s_1, s_2]$, it is convenient to write $F_{s_2,s_1}$for the map which advances the state at s_1 to the state at s_2. For example, if a thyristor is on at time s_1 and off at time s_2, then we write

$$\mathbf{y}(s_2) = F_{s_2,s_1}(\mathbf{x}(s_1)) \tag{6.13}$$

If the thyristor is on during all of the time interval $[s_1, s_2]$, we write F_{s_2,s_1} as $F^{\text{on}}_{s_2,s_1}$. Similarly, if the thyristor is off during all of $[s_1, s_2]$, we write F_{s_2,s_1} as $F^{\text{off}}_{s_2,s_1}$. The formulas for $F^{\text{on}}_{s_2,s_1}$ and $F^{\text{off}}_{s_2,s_1}$ are found by integrating the on and off dynamics (6.2) and (6.5) respectively:

$$F^{\text{on}}_{s_2,s_1}(\mathbf{x}(s_1)) = e^{A_{\text{on}}(s_2-s_1)}\mathbf{x}(s_1) + \int_{s_1}^{s_2} e^{A_{\text{on}}(s_2-s)}B_{\text{on}}u(s)ds \tag{6.14}$$

$$F^{\text{off}}_{s_2,s_1}(\mathbf{y}(s_1)) \;=\; e^{A_{\text{off}}(s_2-s_1)}\mathbf{y}(s_1) + \int_{s_1}^{s_2} e^{A_{\text{off}}(s_2-s)} B_{\text{off}} u(s) ds \tag{6.15}$$

By referring to Figure 6.4, the Poincaré map P may be written in terms of F^{on} and F^{off} and the coordinate changes (6.8) or (6.9) described by Q or R at the switching times:

$$\begin{aligned} P(\mathbf{y}_0) &= F_{t_1,t_0}(\mathbf{y}_0) \\ &= F^{\text{off}}_{t_1,\tau_{1/2}}(R\, F^{\text{on}}_{\tau_{1/2},\phi_{1/2}}(Q\, F^{\text{off}}_{\phi_{1/2},\tau_0}(R\, F^{\text{on}}_{\tau_0,\phi_0}(Q\, F^{\text{off}}_{\phi_0,t_0}(\mathbf{y}_0))))) \end{aligned} \tag{6.16}$$

Different Poincaré maps can be obtained by varying the sample time t_0. One convenient choice is to let t_0 tend to ϕ_0 from below. That is, $t_0 = \phi_0-$. Then the Poincaré map becomes

$$\begin{aligned} P(\mathbf{y}_0) &= F_{\phi_1,\phi_0}(\mathbf{y}_0) \\ &= F^{\text{off}}_{\phi_1,\tau_{1/2}}(R\, F^{\text{on}}_{\tau_{1/2},\phi_{1/2}}(Q\, F^{\text{off}}_{\phi_{1/2},\tau_0}(R\, F^{\text{on}}_{\tau_0,\phi_0}(Q\, \mathbf{y}_0)))) \end{aligned} \tag{6.17}$$

If, instead, t_0 is chosen in the interval $[\phi_0, \tau_0]$ when a thyristor is conducting, then the Poincaré map becomes

$$\begin{aligned} P(\mathbf{x}_0) &= F_{t_1,t_0}(\mathbf{x}_0) \\ &= F^{\text{on}}_{t_1,\phi_1}(Q\, F^{\text{off}}_{\phi_1,\tau_{1/2}}(R\, F^{\text{on}}_{\tau_{1/2},\phi_{1/2}}(Q\, F^{\text{off}}_{\phi_{1/2},\tau_0}(R\, F^{\text{on}}_{\tau_0,t_0}(\mathbf{x}_0))))) \end{aligned} \tag{6.18}$$

Although the Poincaré map P varies with the choice of sample time t_0 (even the dimension of the vectors it acts on varies!), the information that we seek to extract from P such as periodic orbit stability does not depend on the sample time.

6.5 Jacobian of Poincaré map

To study stability, a steady state operating point must be assumed. In a switching circuit this steady state is often periodic. Here we assume that the steady state is periodic with period T. (More precisely, the steady state wave forms, sources and switching times are assumed to be periodic with period T.) Stability analysis of this periodic orbit studies the behavior of the transients which occur when the system is slightly perturbed. Since thyristor switching circuits are nonlinear, the stability depends on the steady state chosen.

We first illustrate the stability computation for a periodic orbit of the simple linear system (6.11). Differentiating (6.12) yields the Jacobian of the Poincaré map $DP = e^{AT}$. This means that a linearized perturbation in state $\delta\mathbf{x}(t_0)$ at time t_0 evolves to a linearized perturbation $\delta\mathbf{x}(t_0+T) = e^{AT}\delta\mathbf{x}(t_0)$ at the end of the period t_0+T. In this case, the stability of the periodic orbit is usually determined by the Jacobian DP and particularly by the eigenvalues of DP: if all the eigenvalues of DP lie inside the unit circle of the complex plane, then the periodic orbit is asymptotically stable. This stability result applies generally to conventional smooth nonlinear systems.

Now consider a regularly fired thyristor circuit which is linear except for the thyristors. Then each thyristor pattern of on or off yields a linear system and the system

switches between these linear systems as the thyristors switch. Although the switch on occurs at a fixed time in the cycle, the switch off time varies during a transient because it depends on the time at which the thyristor current becomes zero. This dependence of the switch off time on the system state makes the thyristor circuit nonlinear. The analysis in the following subsections derives simple and exact formulas for the Jacobian of the Poincaré map. These formulas are assembled simply by multiplying the matrix exponentials which correspond to each linear system and taking account of the varying state space dimension at each switching. The formulas are advantageous both for computations and insight into the stability of thyristor switching circuits.

6.5.1 Thyristor current function and transversality

This subsection defines a thyristor current function f which describes the actual thyristor current while the thyristor is on and the thyristor current that *would have* flowed after the thyristor turn off time *if the thyristor had not turned off*. The thyristor current function is useful for explaining thyristor stability and bifurcation results.

To introduce the thyristor current function f, it is convenient to consider the first half cycle of operation of the SVC example circuit and to assume that the thyristor turn on which begins the half cycle occurs at time zero. At time zero, the thyristor current $I_r(0) = 0$ and the initial state is given by $\mathbf{x}(0) = (0, V_c(0), I_s(0))^{\mathrm{T}}$. The thyristor current function $f(t,p)$ is defined to be the thyristor current assuming the thyristor is on for all time:

$$f(t,p) = (1\ 0\ 0)\left[e^{A_{\mathrm{on}}t}\begin{pmatrix}0\\ V_c(0)\\ I_s(0)\end{pmatrix} + \int_0^t e^{A_{\mathrm{on}}(t-s)}B_{\mathrm{on}}u(s)ds\right] \tag{6.19}$$

Note that $f(0,p) = 0$. p denotes parameters of the SVC circuit; the dependence of f on p is used to describe switching time bifurcations in the following sections.

The thyristor current function $f(t,p)$ can be used to describe the thyristor switch off rule precisely. If the thyristor switches on at $t = 0$, then the thyristor will switch off at the *first positive* root τ of f:

$$\tau = \min\{\ t \mid f(t,p) = 0,\ t > 0\} \tag{6.20}$$

In particular, the switch off time τ satisfies

$$0 = f(\tau, p) \tag{6.21}$$

If the slope of the thyristor current is negative at the turn off time so that

$$\left.\frac{\partial f}{\partial t}\right|_{\tau,p} < 0 \tag{6.22}$$

then the turn off is called *transversal*. (A transversal turn off is a simple root of f.) The transversality condition (6.22) can also be written in terms of the actual thyristor current I_r as

$$\left.\frac{dI_r}{dt}\right|_{\tau-} < 0 \tag{6.23}$$

where $\tau-$ denotes a limit taken from the left hand side of τ.

If a switch off is transversal at time τ, then sufficiently small variations in initial conditions or circuit parameters cause a switch off time near to τ and this switch off time is a smooth function of small variations in initial conditions or circuit parameters. (This is proved in [5]: it is apparent that the transversal root of f near τ is preserved under sufficiently small variations, but it must also be checked that sufficiently small variations prevent any *new* roots of f occurring before the switch off near τ; according to (6.20), any such root would become the first root of f for $t > 0$ and the thyristor switch off time.)

Transversality at all the switch offs in a periodic steady state is essential for computing the Jacobian of the Poincaré map. On the other hand, the transversality condition (6.22) fails when $\frac{\partial f}{\partial t}|_{\tau,p} = 0$ at a switch off and in this case it is typical for switching times to jump or bifurcate and steady state stability to be lost as explained in section 6.7.1.

6.5.2 Relations between on and off systems

The matrices R and Q were introduced in section 6.3 to change the dimension of the state of the SVC example circuit at switchings and are

$$R = \begin{pmatrix} 0 & 1 & 0 \\ 0 & 0 & 1 \end{pmatrix} \qquad \text{and} \qquad Q = R^{\mathrm{T}} = \begin{pmatrix} 0 & 0 \\ 1 & 0 \\ 0 & 1 \end{pmatrix} \tag{6.24}$$

This subsection shows how R and Q relate the on and off system dynamics and also their relation to the thyristor switch off condition. These relationships are shown here only for the SVC example circuit, but this example accurately reflects structural properties of general thyristor and diode circuits [5].

The on and off system dynamics are specified in section 6.3 using

$$A_{\text{on}} = \begin{pmatrix} -R_r/L_r & 1/L_r & 0 \\ -1/C & 0 & 1/C \\ 0 & -1/L_s & -R_s/L_s \end{pmatrix} \text{ and } B_{\text{on}} = \begin{pmatrix} 0 \\ 0 \\ 1/L_s \end{pmatrix}, \tag{6.25}$$

$$A_{\text{off}} = \begin{pmatrix} 0 & 1/C \\ -1/L_s & -R_s/L_s \end{pmatrix} \text{ and } B_{\text{off}} = \begin{pmatrix} 0 \\ 1/L_s \end{pmatrix} \tag{6.26}$$

It is easy to check that

$$A_{\text{off}} = RA_{\text{on}}Q \qquad \text{and} \qquad B_{\text{off}} = RB_{\text{on}} \tag{6.27}$$

The thyristor switch off condition is zero thyristor current:

$$0 = I_r(\tau) \tag{6.28}$$

and this switch off condition may be written in terms of the state $\mathbf{x}$ using the row vector $c = (\,1 \quad 0 \quad 0\,)$:

$$0 = (\,1 \quad 0 \quad 0\,) \begin{pmatrix} I_r(t) \\ V_c(t) \\ I_s(t) \end{pmatrix} = c\,\mathbf{x}(\tau) \tag{6.29}$$

The connection between c and R and Q may be shown by computing

$$\begin{aligned} I - QR &= \begin{pmatrix} 1 & 0 & 0 \\ 0 & 1 & 0 \\ 0 & 0 & 1 \end{pmatrix} - \begin{pmatrix} 0 & 0 \\ 1 & 0 \\ 0 & 1 \end{pmatrix} \begin{pmatrix} 0 & 1 & 0 \\ 0 & 0 & 1 \end{pmatrix} \\ &= \begin{pmatrix} 1 & 0 & 0 \\ 0 & 0 & 0 \\ 0 & 0 & 0 \end{pmatrix} = \begin{pmatrix} 1 \\ 0 \\ 0 \end{pmatrix} \begin{pmatrix} 1 & 0 & 0 \end{pmatrix} = c^{\mathrm{T}} c \end{aligned} \tag{6.30}$$

Relationships (6.27) and (6.30) underpin useful simplifications of the Jacobian formulas in the next section.

6.5.3 Derivation of Jacobian formula

We now derive a simple formula for the Poincaré map Jacobian of a periodic orbit. The approach is to divide one period of operation into subintervals, each of which contains one thyristor switching and to compute the Jacobian of the map which advances the state from the beginning to the end of each subinterval. Then the chain rule is used to compute the Jacobian of the Poincaré map as the product of the Jacobians for the subintervals. It is assumed that the thyristor turns on when the firing pulse is applied; that is, there are no thyristor misfires.

Interval containing a switch on

Let $[s_2, s_3]$ be a time interval including a thyristor switch on at time ϕ and no other switchings. We write F_{s_3,s_2} for the flow which maps the initial state $\mathbf{y}(s_2)$ at s_2 to the final state $\mathbf{x}(s_3)$ at s_3 so that

$$\mathbf{x}(s_3) = F_{s_3,s_2}\left(\mathbf{y}(s_2)\right) \tag{6.31}$$

In general the switch on time ϕ is a function of the initial state $\mathbf{y}(s_2)$ and we write this (with some abuse of notation) as $\phi = \phi(\mathbf{y}(s_2))$. We now compute F_{s_3,s_2} and its Jacobian DF_{s_3,s_2} with respect to $\mathbf{y}(s_2)$.

The thyristor is off in $[s_2, \phi]$ so that integrating the off system equations (6.5) yields

$$\mathbf{y}(\phi) = F^{\mathrm{off}}_{\phi,s_2}(\mathbf{y}(s_2)) = e^{A_{\mathrm{off}}(\phi - s_2)} \left(\mathbf{y}(s_2) + \int_{s_2}^{\phi} e^{A_{\mathrm{off}}(s_2 - s)} B_{\mathrm{off}} u(s) ds \right) \tag{6.32}$$

The equation transforming to the $\mathbf{x}$ coordinates at ϕ is

$$\mathbf{x}(\phi) = Q\mathbf{y}(\phi) \tag{6.33}$$

The thyristor is on in $[\phi, s_3]$ so that integrating the on system equations (6.2) and using (6.33) yields

$$F_{s_3,s_2}\left(\mathbf{y}(s_2)\right) = F^{\mathrm{on}}_{s_3,\phi}\left(\mathbf{x}(\phi)\right) = e^{A_{\mathrm{on}}(s_3 - \phi)} Q\mathbf{y}(\phi) + \int_{\phi}^{s_3} e^{A_{\mathrm{on}}(s_3 - s)} B_{\mathrm{on}} u(s) ds \tag{6.34}$$

Substitute from (6.32) to obtain

$$F_{s_3,s_2}\left(\mathbf{y}(s_2)\right) = G_{s_3,s_2}\left(\mathbf{y}(s_2), \phi(\mathbf{y}(s_2))\right) \tag{6.35}$$

where

$$\begin{aligned} G_{s_3,s_2}\left(\mathbf{y}(s_2), \phi\right) = {} & e^{A_{\text{on}}(s_3-\phi)} Q\, e^{A_{\text{off}}(\phi-s_2)} \left(\mathbf{y}(s_2) + \int_{s_2}^{\phi} e^{A_{\text{off}}(s_2-s)} B_{\text{off}} u(s) ds\right) \\ & + \int_{\phi}^{s_3} e^{A_{\text{on}}(s_3-s)} B_{\text{on}} u(s) ds \end{aligned} \tag{6.36}$$

Differentiating (6.35) and writing D for derivative with respect to $\mathbf{y}(s_2)$ gives

$$DF_{s_3,s_2} = DG_{s_3,s_2} + \frac{\partial G_{s_3,s_2}}{\partial \phi} D\phi \tag{6.37}$$

$D\phi$ is the derivative of the switch off time with respect to $\mathbf{y}(s_2)$. In this section we make the simplifying assumption that the thyristor is fired regularly; that is, ϕ is constant, and hence $D\phi = 0$ and

$$DF_{s_3,s_2} = DG_{s_3,s_2} = e^{A_{\text{on}}(s_3-\phi)} Q e^{A_{\text{off}}(\phi-s_2)} \tag{6.38}$$

(The case of thyristor firing control or synchronization is briefly treated in section 6.9.)

Interval containing a switch off

Let $[s_1, s_2]$ be a time interval including a single transversal thyristor switch off at time τ and no other switchings. Write F_{s_2,s_1} for the flow which maps the state at s_1 to the state at s_2 so that

$$\mathbf{y}(s_2) = F_{s_2,s_1}\left(\mathbf{x}(s_1)\right) \tag{6.39}$$

The switch off time τ is a function of the initial state $\mathbf{x}(s_1)$ and we write this as $\tau = \tau(\mathbf{x}(s_1))$. We now compute F_{s_2,s_1} and its Jacobian DF_{s_2,s_1} with respect to $\mathbf{x}(s_1)$.

The thyristor is on in $[s_1, \tau]$ so that integrating the on system equations (6.2) yields

$$\mathbf{x}(\tau) = F^{\text{on}}_{\tau,s_1}(x(s_1)) = e^{A_{\text{on}}(\tau-s_1)} \left(\mathbf{x}(s_1) + \int_{s_1}^{\tau} e^{A_{\text{on}}(s_1-s)} B_{\text{on}} u(s) ds\right) \tag{6.40}$$

The transformation to $\mathbf{y}$ coordinates at the switch off time τ is

$$\mathbf{y}(\tau) = R\,\mathbf{x}(\tau) \tag{6.41}$$

The thyristor is off in $[\tau, s_2]$ so that integrating the off system equations (6.5) with initial condition $\mathbf{y}(\tau)$ gives

$$F_{s_2,s_1}\left(\mathbf{x}(s_1)\right) = F^{\text{off}}_{\tau,s_1}(\mathbf{y}(\tau)) = e^{A_{\text{off}}(s_2-\tau)}\, R\,\mathbf{x}(\tau) + \int_{\tau}^{s_2} e^{A_{\text{off}}(s_2-s)} B_{\text{off}} u(s) ds \tag{6.42}$$

Substituting for $\mathbf{x}(\tau)$ from (6.40) yields

$$F_{s_2,s_1}\left(\mathbf{x}(s_1)\right) = G_{s_2,s_1}\left(\mathbf{x}(s_1), \tau(\mathbf{x}(s_1))\right) \tag{6.43}$$

where

$$G_{s_2,s_1}(\mathbf{x}(s_1),\tau) = e^{A_{\rm off}(s_2-\tau)} R e^{A_{\rm on}(\tau-s_1)} \left(\mathbf{x}(s_1) + \int_{s_1}^{\tau} e^{A_{\rm on}(s_1-s)} B_{\rm on} u(s) ds \right) + \int_{\tau}^{s_2} e^{A_{\rm off}(s_2-s)} B_{\rm off} u(s) ds \tag{6.44}$$

The transversality of the switch off was assumed above and it implies that τ is a smooth function of $\mathbf{x}(s_1)$ [5] and hence that F_{s_2,s_1} is a smooth function of $\mathbf{x}(s_1)$. Differentiating (6.43) and writing D for derivative with respect to $\mathbf{x}(s_1)$ gives

$$DF_{s_2,s_1} = DG_{s_2,s_1} + \frac{\partial G_{s_2,s_1}}{\partial \tau} D\tau \tag{6.45}$$

Differentiating (6.44) yields

$$\begin{aligned} \frac{\partial G_{s_2,s_1}}{\partial \tau} &= e^{A_{\rm off}(s_2-\tau)} (RA_{\rm on} - A_{\rm off} R)\, e^{A_{\rm on}(\tau-s_1)} \left(\mathbf{x}(s_1) + \int_{s_1}^{\tau} e^{A_{\rm on}(s_1-s)} B_{\rm on} u(s) ds \right) \\ &\quad + e^{A_{\rm off}(s_2-\tau)} (RB_{\rm on} - B_{\rm off}) u(\tau) \\ &= e^{A_{\rm off}(s_2-\tau)} (RA_{\rm on} - A_{\rm off} R)\, \mathbf{x}(\tau) + e^{A_{\rm off}(s_2-\tau)} (RB_{\rm on} - B_{\rm off}) u(\tau) \end{aligned} \tag{6.46}$$

But the structural relations (6.27) in section 6.5.2 state that $B_{\rm off} = RB_{\rm on}$ and $A_{\rm off} = RA_{\rm on}Q$ so that

$$\frac{\partial G_{s_2,s_1}}{\partial \tau} = e^{A_{\rm off}(s_2-\tau)} RA_{\rm on}(I - QR)\, \mathbf{x}(\tau) \tag{6.47}$$

Using the relation (6.30) linking $I - QR$ and $c = (\,1 \quad 0 \quad 0\,)$ from section 6.5.2,

$$\begin{aligned} \frac{\partial G_{s_2,s_1}}{\partial \tau} &= e^{A_{\rm off}(s_2-\tau)} RA_{\rm on} c^{\rm T} c\, \mathbf{x}(\tau) \\ &= 0 \end{aligned} \tag{6.48}$$

since the thyristor switch off condition is $0 = I_r(\tau) = (\,1 \quad 0 \quad 0\,)\, \mathbf{x}(\tau) = c\,\mathbf{x}(\tau)$. Equation (6.48) states that the final state $y(s_2)$ is independent of the switch off time τ to first order!

Hence we obtain the surprising and simple result

$$DF_{s_2,s_1} = DG_{s_2,s_1} = e^{A_{\rm off}(s_2-\tau)} R e^{A_{\rm on}(\tau-s_1)} \tag{6.49}$$

Assembling the Jacobian

The Poincaré map formula (6.16) is rewritten omitting the thicket of brackets:

$$\begin{aligned} P(\mathbf{y}_0) &= F^{\rm off}_{t_1,\tau_{1/2}} (R\, F^{\rm on}_{\tau_{1/2},\phi_{1/2}} (Q\, F^{\rm off}_{\phi_{1/2},\tau_0} (R\, F^{\rm on}_{\tau_0,\phi_0} (Q\, F^{\rm off}_{\phi_0,t_0} (\mathbf{y}_0))))) \\ &= F^{\rm off}_{t_1,\tau_{1/2}} R\, F^{\rm on}_{\tau_{1/2},\phi_{1/2}} Q\, F^{\rm off}_{\phi_{1/2},\tau_0} R\, F^{\rm on}_{\tau_0,\phi_0} Q\, F^{\rm off}_{\phi_0,t_0}\, \mathbf{y}_0 \end{aligned} \tag{6.50}$$

Choose times s_2 in the interval $(\phi_{1/2}, \tau_{1/2})$, s_1 in $(\tau_0, \phi_{1/2})$, and s_0 in (ϕ_0, τ_0). Then

$$P(\mathbf{y}_0) = F_{t_1,s_2} F_{s_2,s_1} F_{s_1,s_0} F_{s_0,t_0}\, \mathbf{y}_0 \tag{6.51}$$

Each of the time intervals corresponding to the decomposition of the Poincaré map in (6.51) contains exactly one switching. Differentiating (6.51) with the chain rule and using the results of sections 6.5.3 and 6.5.3 gives

$$\begin{aligned} DP &= DF_{t_1,s_2} DF_{s_2,s_1} DF_{s_1,s_0} DF_{s_0,t_0} \\ &= \left(e^{A_{\text{off}}(t_1-\tau_{1/2})} R e^{A_{\text{on}}(\tau_{1/2}-s_2)}\right) \left(e^{A_{\text{on}}(s_2-\phi_{1/2})} Q e^{A_{\text{off}}(\phi_{1/2}-s_1)}\right) \\ &\quad \left(e^{A_{\text{off}}(s_1-\tau_0)} R e^{A_{\text{on}}(\tau_0-s_0)}\right) \left(e^{A_{\text{on}}(s_0-\phi_0)} Q e^{A_{\text{off}}(\phi_0-t_0)}\right) \\ &= e^{A_{\text{off}}(t_1-\tau_{1/2})} R e^{A_{\text{on}}(\tau_{1/2}-\phi_{1/2})} Q e^{A_{\text{off}}(\phi_{1/2}-\tau_0)} R e^{A_{\text{on}}(\tau_0-\phi_0)} Q e^{A_{\text{off}}(\phi_0-t_0)} \end{aligned} \tag{6.52}$$

If, for convenience, the sample time of the Poincaré map is changed so that $t_0 = \phi_0-$, then the Jacobian becomes

$$DP = e^{A_{\text{off}}(\phi_1-\tau_{1/2})} R e^{A_{\text{on}}(\tau_{1/2}-\phi_{1/2})} Q e^{A_{\text{off}}(\phi_{1/2}-\tau_0)} R e^{A_{\text{on}}(\tau_0-\phi_0)} Q \tag{6.53}$$

If the sample time t_0 is chosen when a thyristor is on so that, for example, $t_0 = \phi_0+$, then the Jacobian becomes

$$DP = Q e^{A_{\text{off}}(\phi_1-\tau_{1/2})} R e^{A_{\text{on}}(\tau_{1/2}-\phi_{1/2})} Q e^{A_{\text{off}}(\phi_{1/2}-\tau_0)} R e^{A_{\text{on}}(\tau_0-\phi_0)} \tag{6.54}$$

The Jacobian in (6.54) has one more row and column than the Jacobian in (6.53). However, it can be shown that (6.54) and (6.53) have the same eigenvalues except that (6.54) has an additional zero eigenvalue. Thus (6.54) and (6.53) describe exactly the same periodic orbit stability information in different forms.

6.5.4 Discussion of Jacobian formula

We summarize the outcome of the preceding subsections in deriving the Poincaré map Jacobian for the SVC circuit example. The thyristor firing pulses and hence, assuming no misfire, the thyristor switch on times are assumed to occur at fixed times ϕ_0 and $\phi_{1/2}$ in the cycle. It is convenient to choose the Poincaré map sample time at the turn on ϕ_0. Then the Poincaré map P advances the state $\mathbf{y}(\phi_0)$ at turn on to $P(\mathbf{y}) = \mathbf{y}(\phi_0 + T)$, where T is the period. A thyristor switches off at τ_0 and $\tau_{1/2}$ and these switchings are assumed to be transversal in order to guarantee that the Poincaré map is differentiable. The Jacobian of the Poincaré map is

$$DP = e^{A_{\text{off}}(\phi_1-\tau_{1/2})} R e^{A_{\text{on}}(\tau_{1/2}-\phi_{1/2})} Q e^{A_{\text{off}}(\phi_{1/2}-\tau_0)} R e^{A_{\text{on}}(\tau_0-\phi_0)} Q \tag{6.55}$$

Suppose that the circuit has a periodic orbit passing through $\mathbf{y}_0$ at time ϕ_0 so that $\mathbf{y}_0$ is a fixed point of P and $P(\mathbf{y}_0) = \mathbf{y}_0$. The stability of the periodic orbit is the same as the stability of $\mathbf{y}_0$ and is given (except in marginal cases) by the eigenvalues of DP, the Jacobian of the Poincaré map evaluated at $\mathbf{y}_0$. (Here we continue to assume that there are no misfires and that all switch offs are transversal.)

One of the interesting and useful consequences of formula (6.55) is that DP and the stability of the periodic orbit only depend on the state and the input via the

thyristor nonconduction times $\phi_1 - \tau_{1/2}$ and $\phi_{1/2} - \tau_0$ and the thyristor conduction times $\tau_{1/2} - \phi_{1/2}$ and $\tau_0 - \phi_0$. It is remarkable that (6.55) is also the formula that would be obtained for fixed switch off times τ_0 and $\tau_{1/2}$; the varying switch off times introduce no additional complexity in the formula, but the nonlinearity of the circuit is clear since τ_0 and $\tau_{1/2}$ vary as a function of the periodic orbit.

If the periodic orbit is assumed to be half wave symmetric, then $\phi_{1/2} = \phi_0 + T/2$ and $\tau_{1/2} = \tau_0 + T/2$ and (6.55) simplifies to

$$DP = \left(e^{A_{\text{off}}(\phi_{1/2}-\tau_0)} R e^{A_{\text{on}}(\tau_0-\phi_0)} Q\right)^2 \tag{6.56}$$

which can also be expressed in terms of the thyristor conduction time $\sigma = \tau_0 - \phi_0$ as

$$DP = \left(e^{A_{\text{off}}(T/2-\sigma)} R e^{A_{\text{on}}\sigma} Q\right)^2 \tag{6.57}$$

The action of (6.57) on a linearized perturbation $\delta\mathbf{y}$ for the first half period may be informally described as follows: change to $\mathbf{x}$ coordinates with the matrix Q, let the on system act for time σ, project to the off coordinates with the matrix R and let the off system act for time $T/2 - \sigma$. The action of (6.57) on $\delta\mathbf{y}$ for the whole period is equivalent to the action of two successive half periods.

6.6 Switching damping

This section analyzes thyristor switch off as a source of damping. This damping is a dynamic effect which damps transients; the effect has nothing to do with static or steady state performance. The switching damping occurs in addition to other sources of circuit damping such as resistance or control loops. In particular, switching damping occurs in regularly fired thyristor circuits with no resistance or control loop.

6.6.1 Simple example

The damping caused by thyristor switch off can be most easily demonstrated in an example from [15]: Consider the circuit of Figure 6.5 which consists of a sinusoidal voltage source, a thyristor fired regularly once a period and an inductor all in series. This example is simple, but does contain the essence of the switching damping phenomenon in general thyristor circuits.

The periodic steady state $I(t)$ of the circuit current is shown by the gray line in Figure 6.6. If there is a disturbance ϵ which perturbs the current I at time zero, then a transient $I(t) + \Delta I(t)$ with $\Delta I(0) = \epsilon$ ensues as shown by the solid line in the upper portion of Figure 6.6. The transient persists until shortly after the thyristor switches off at time τ_0. It is clear that by the next period, the transient has been damped to nothing. That is, the Poincaré map P zeros the disturbance:

$$P(I(0) + \epsilon) = I(0) \tag{6.58}$$

(In discrete time control, this would be called deadbeat damping.)

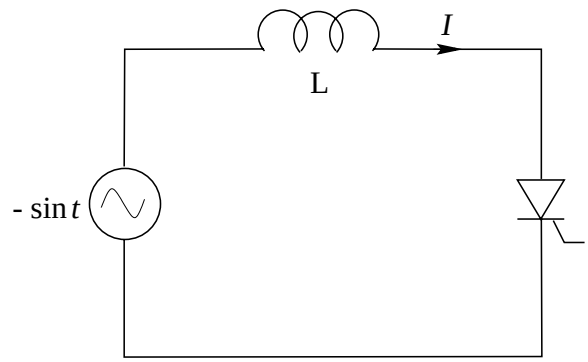

Figure 6.5: Simple thyristor circuit showing switching damping.

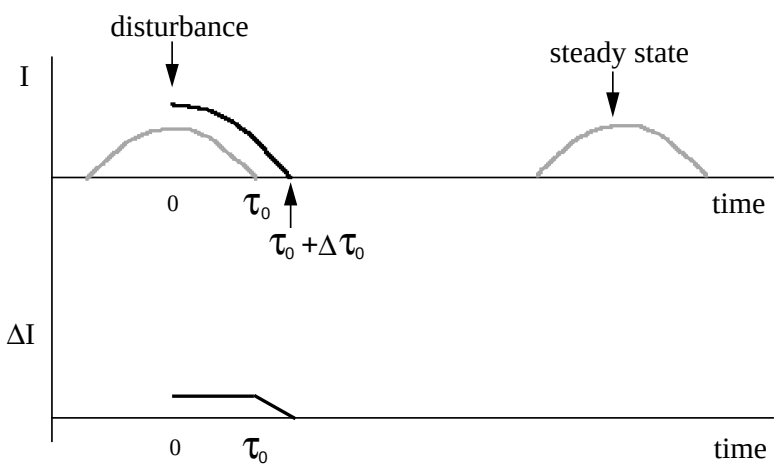

Figure 6.6: Damping of a disturbance $\Delta I(t)$ in simple thyristor circuit.

Computing the Poincaré map Jacobian confirms the analysis: The on equation has one state I in the one dimensional state space $\mathbb{R}$ and is $\dot{I} = -\sin t$. The off equation has the degenerate, zero dimensional state space $\mathbb{R}^0 = \{0\}$ which consists only of the origin. Thus, as expected, $I = 0$ when the thyristor is off. Since $R = 0$, the Jacobian calculation yields $DP = e^{A_{\text{on}}\tau_0} R\, e^{A_{\text{off}}(T-\tau_0)} = 0$.

The size of the disturbance $\Delta I(t)$ is given by the difference between the disturbed trajectory and the steady state. It is this difference which is damped to zero. To see how the thyristor switch off accomplishes the damping, observe that the disturbance remains constant until the thyristor of the steady state trajectory switches off; the disturbance is damped to zero during the time in which the thyristor of the disturbed trajectory is on and the thyristor of the steady state trajectory is off.

One might be tempted to neglect the change in state space dimension in the problem formulation; that is, to assume that the off equation was $\dot{I} = 0$ with I in the

one dimensional state space $\mathbb{R}$ and neglect the projection R. After all, the periodic solution can be calculated correctly with this formulation since I is zero at the beginning of the switch off mode. However, in this formulation, linearizing either the on equation or the off equation gives $\dot{\delta I} = 0$ and the solution is $\delta I(t) = \delta I(0)$. This implies that, to first order, the disturbance is preserved and not damped at the end of the cycle (that is, $DP = 1$). This is plainly wrong. Essentially the same mistake of neglecting the change in state space dimension can be made in general thyristor and diode circuits. For another example, see section 6.8.2.

6.6.2 Switching damping in the SVC example

We compute damping in the SVC example circuit with the thyristor conduction time σ treated as a parameter. A halfwave symmetric periodic steady state is assumed. Then, according to (6.57), the Poincaré map Jacobian is given by

$$DP = (DH)^2 \tag{6.59}$$

where

$$DH = e^{A_{\text{off}}(T/2-\sigma)} R e^{A_{\text{on}}\sigma} Q \tag{6.60}$$

H may be regarded as the map $F_{\phi+T/2,\phi}$ advancing the state by half a period:

$$\mathbf{y}(\phi + T/2) = H(\mathbf{y}(\phi)) = F_{\phi+T/2,\phi}(\mathbf{y}(\phi)) \tag{6.61}$$

Since the eigenvalues of DP are the eigenvalues of DH squared, the eigenvalues of DH determine the stability of periodic orbits of the circuit.

It is straightforward to use (6.60) to compute the locus of eigenvalues of DH as σ varies over its range of 0 to 180 degrees and the results are shown in Figure 6.7(a). (The gap in results for $60^o < \sigma < 90^o$ is due to the switching time bifurcations explained in section 6.7.1; the halfwave symmetric periodic orbit disappears in this range.)

When all the eigenvalues are inside the unit circle, the circuit periodic orbit is asymptotically stable and the system damps out any small perturbations. This damping cannot be entirely attributed to resistance in the circuit. Indeed, if the circuit resistances are set to zero then the eigenvalue locus of Figure 6.7(b) is obtained and the switching damping for most values of σ is evident. (The exceptional points on the unit circle of zero damping are due to a resonance effect explained in [4].)

6.6.3 Variational equation

We consider the first order variation [2] about periodic orbits to get another view of how the Poincaré map Jacobian works. The first order variation is a linear differential equation which propagates forward in time linearized deviations from the periodic orbit. Propagation with the variational equation of an initial linearized deviation for one period T is equivalent to the action of the Poincaré map Jacobian on the initial linearized deviation.

First we examine the first order variation for the simple example circuit shown in Figure 6.5. Write τ_0 for the switch off time of the steady state trajectory $I(t)$ and

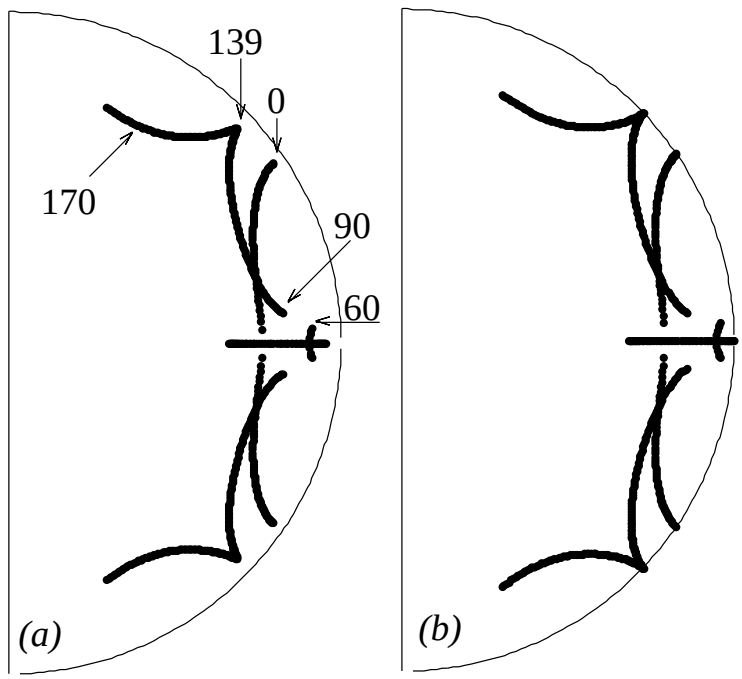

Figure 6.7: Eigenvalues of DH: (a) Circuit with resistance, (b) without resistance. The numbers show the thyristor conduction time σ in degrees.

$\tau_0 + \Delta\tau_0$ for the switch off time of the disturbed trajectory $I(t) + \Delta I(t)$ as shown in Figure 6.6. Here Δ denotes deviation; shortly we will use δ to denote linearized deviation. By inspection,

$$\Delta I(t) = \begin{cases} \epsilon & ; \quad 0 \le t \le \tau_0 \\ 0 & ; \quad \tau_0 + \Delta\tau_0 \le t \end{cases} \tag{6.62}$$

Since $\Delta\tau_0 \to 0$ as $\epsilon \to 0$,

$$\left.\frac{\partial \Delta I(t)}{\partial \epsilon}\right|_{\epsilon=0} = \begin{cases} 1 & ; \quad 0 \le t \le \tau_0 \\ 0 & ; \quad \tau_0 < t \end{cases} \tag{6.63}$$

and (6.63) is the solution to the variational equation when the initial disturbance is 1. The general solution $\delta I(t)$ to the variational equation when the initial disturbance is $\delta I(0)$ is

$$\delta I(t) = \begin{cases} \delta I(0) & ; \quad 0 \le t \le \tau_0 \\ 0 & ; \quad \tau_0 < t \end{cases} \tag{6.64}$$

The zeroing of the linearized disturbance $\delta I(0)$ at switch off τ_0 in (6.64) corresponds exactly to the action of the projection R in the Poincaré map formula. A circuit model

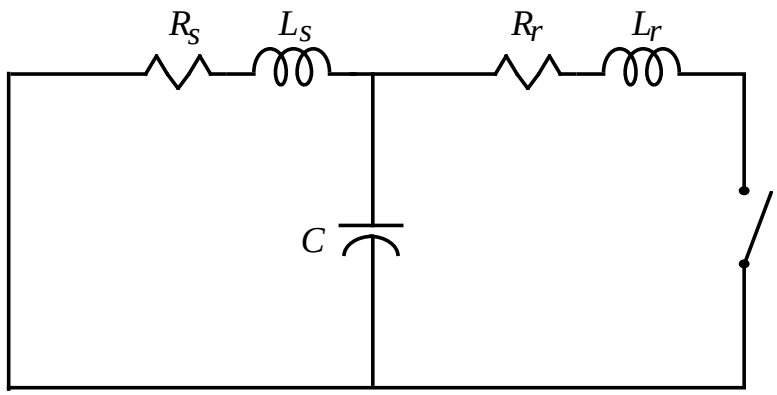

Figure 6.8: Circuit model for the variational equations.

of the variational equation is the inductor of the simple circuit in series with an ideal switch which opens and zeros the current at time τ_0.

Now we consider the variational equation of the SVC circuit about a half wave symmetric periodic orbit. The linearized deviations propagated by the variational equations are $\delta\mathbf{x}(t) = (\delta I_r(t), \delta V_c(t), \delta I_s(t))^{\mathrm{T}}$ and $\delta\mathbf{y}(t) = (\delta V_c(t), \delta I_s(t))^{\mathrm{T}}$. The variational equations for the first half period are

$$\delta\mathbf{x}(\phi_0) = Q\delta\mathbf{y}(\phi_0) \quad \text{(switch opening at } \phi_0) \tag{6.65}$$

$$\dot{\delta\mathbf{x}} = A_{\mathrm{on}}\delta\mathbf{x} \quad \text{(switch closed)} \tag{6.66}$$

$$\delta\mathbf{y}(\tau_0) = R\delta\mathbf{x}(\tau_0) \quad \text{(switch closing at } \tau_0) \tag{6.67}$$

$$\dot{\delta\mathbf{y}} = A_{\mathrm{off}}\delta\mathbf{y} \quad \text{(switch open)} \tag{6.68}$$

and these equations are repeated for the second half cycle. Integrating the variational equations over one half cycle produces the Jacobian of the half wave map H:

$$DH = e^{A_{\mathrm{off}}(T/2-\sigma)} R e^{A_{\mathrm{on}}\sigma} Q \tag{6.69}$$

and integrating the variational equations over one complete cycle produces DP, the Jacobian of the Poincaré map:

$$DP = \left(e^{A_{\mathrm{off}}(T/2-\sigma)} R e^{A_{\mathrm{on}}\sigma} Q\right)^2 \tag{6.70}$$

A circuit model of the variational equations is shown in Figure 6.8; it is obtained from the SVC example circuit by shorting the source and replacing the thyristor by an ideal switch which opens at times τ_0 and $\tau_{1/2}$. In general the switch current is nonzero when the switch opens at τ_0 and the switch opening is assumed to immediately zero the inductor current. This somewhat nonphysical event is described in (6.67) by the projection of the current $\delta\mathbf{x}(\tau_0)$ onto the plane $\delta I_r = 0$ by R. This projection or ideal switch opening is the source of switching damping.

We consider the case of zero resistances so that equations (6.66) and (6.68) are simply lossless oscillators. At the beginning of the cycle the switch turns on and the

on oscillation proceeds for time σ. Then the state is projected onto the plane of zero thyristor current and the off oscillation proceeds for time $T/2 - \sigma$. Since we have assumed zero resistance, the oscillators are lossless and the damping in DH is entirely accounted for by the projection onto the plane of zero thyristor current.

It is straightforward to use an energy or Lyapunov method to show that DH is never unstable and that its eigenvalues always lie inside or on the unit circle. Consider the incremental energy [5, 26, 28]

$$\delta E(t) = \frac{1}{2}L_r(\delta I_r)^2 + \frac{1}{2}L_s(\delta I_s)^2 + \frac{1}{2}C(\delta V_c)^2 \tag{6.71}$$

δE measures the square of the size of the perturbation $(\delta I_r, \delta I_s, \delta V_c)^{\mathrm{T}}$. δE is preserved at the switch opening (6.65) because the reactor current δI_r is zero when the switch opens (the first component of $Q\delta\mathbf{y}(\phi_0)$ is always zero). At the switch closing (6.68), the incremental energy δE decreases by the nonnegative quantity $\frac{1}{2}L_r\left(\delta I_r(\tau_0)\right)^2$ because the effect of the projection R is to zero the incremental thyristor current δI_r.

In the case of zero circuit resistances, equations (6.66) and (6.68) are simply lossless oscillators. Then δE is preserved at switch on, is constant while the lossless oscillators act and decreases or is preserved at switch off. Since δE is a Lyapunov function for the discrete time system $\delta\mathbf{y}^{k+1} = DH\delta\mathbf{y}^k$, $k = 0, 1, 2, 3...$, DH must be stable. If the circuit resistances are included, then δE is strictly decreasing when the oscillators act and δE is a strict Lyapunov function and DH is asymptotically stable. The stability or asymptotic stability of DP follows from the stability or asymptotic stability of DH.

In summary, for the case of no resistance we have shown stability of DP by Lyapunov methods and for the case of circuit resistance we have shown asymptotic stability of DP both by direct calculation of the eigenvalues and by Lyapunov methods. It would now seem routine for the case of circuit resistance to conclude from the Jacobian asymptotic stability that the periodic orbit is always asymptotically stable. However, this conclusion is false: the periodic orbit can sometimes lose stability! The following section explains how this happens.

6.7 Switching time bifurcations

6.7.1 Switching time bifurcations and instability

This subsection explains how switching time bifurcations cause a loss of steady state stability.

Thyristor switching circuits initially operating at a periodic orbit can lose stability when switching times jump or bifurcate as a parameter is slowly varied. One example of such a parameter is the conduction time σ of the thyristor. (σ for a periodic orbit can be varied by varying the thyristor firing time.)

The switching time bifurcations can be explained using the thyristor current function. It is convenient to assume that a thyristor turns on at time zero. Recall from section 6.5.1 that the thyristor current function $f(t, \sigma)$ is defined to be the thyristor current assuming the thyristor is on for all time. In the case of the SVC circuit

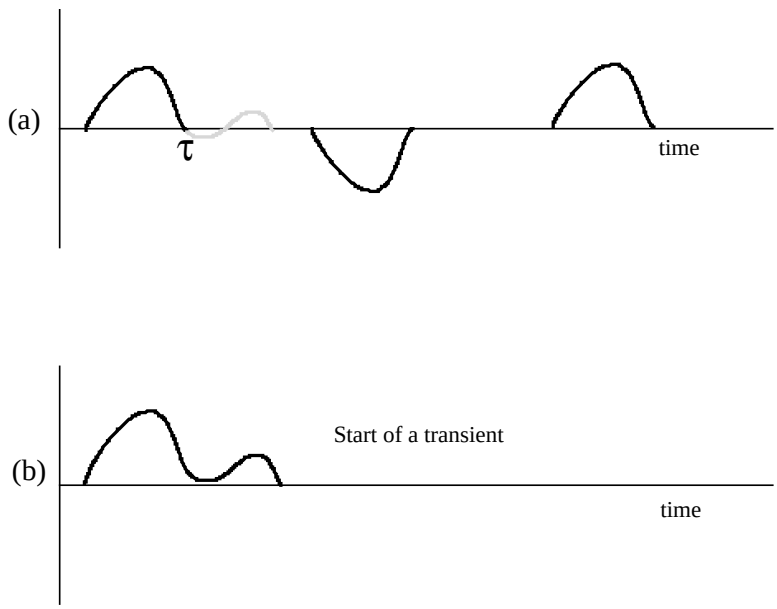

Figure 6.9: Two thyristor current zeros disappear (a) $\sigma < \sigma^*$, (b) $\sigma \approx \sigma^*, \sigma > \sigma^*$

example,

$$f(t,\sigma) = (1\ 0\ 0)\left[e^{A_{\text{on}}t}\begin{pmatrix}0\\ V_c(0)\\ I_s(0)\end{pmatrix} + \int_0^t e^{A_{\text{on}}(t-\tau)}B_{\text{on}}u(\tau)d\tau\right] \tag{6.72}$$

It is important to remember that the thyristor current function is identical to the actual thyristor current before the switch off τ and a useful mathematical fiction after the switch off τ.

If the thyristor turns on at time zero, the next thyristor switch off time is at the *first* positive root τ of f. Switching time bifurcations are bifurcations of the roots of f which alter which root is the first positive root. The switching time bifurcations occur in practice when the harmonic components of the thyristor current are large and the thyristor current function becomes distorted [14].

Figure 6.9 explains a switching time bifurcation in which the periodic orbit loses stability as a thyristor current zero disappears. Figure 6.9a shows the thyristor current function for a stable periodic solution; there is a transversal switch off at time τ. As the thyristor conduction time σ is slowly varied, the dip in the thyristor current function after τ rises until, passing through the critical parameter value σ^*, the current zero disappears and a new, later zero of the thyristor current applies (see Figure 6.9b). The switch off time of the thyristor has suddenly increased in a switching time bifurcation and stability has suddenly been lost. As soon as the switching time bifurcates and system stability is lost, a transient starts.

Another manifestation of a switching time bifurcation is shown in Figure 6.10.

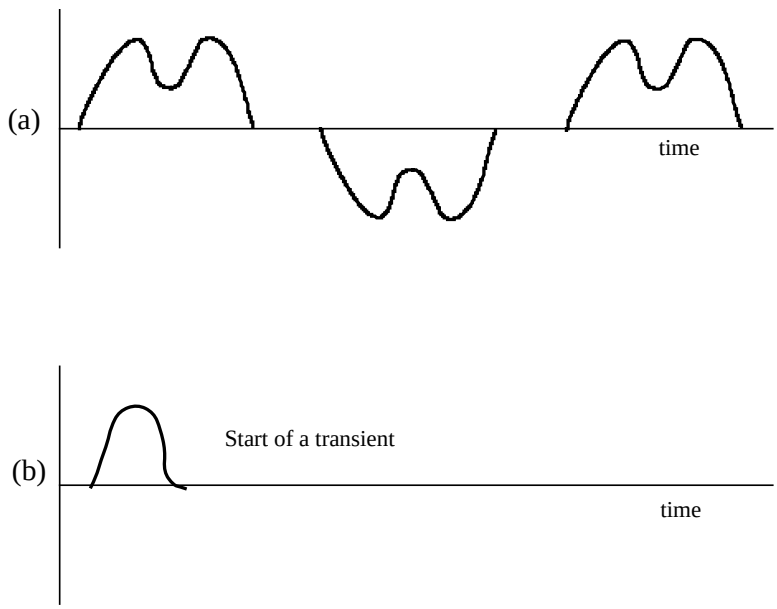

Figure 6.10: A new earlier thyristor current zero appears (a) $\sigma > \sigma^*$, (b) $\sigma = \sigma^*$

Suppose that harmonic distortion produces a dip in the thyristor current as shown in Figure 6.10a. The periodic steady state is stable in Figure 6.10a. As the thyristor conduction time σ is varied, the dip lowers until, at a critical parameter value σ^*, a new, earlier zero of the thyristor current is produced (Figure 6.10b). The switch off time of the thyristor suddenly decreases and the stable operation of the system at the previous periodic steady state is lost. As soon as the switching time bifurcates, a transient starts.

In both Figure 6.9 and 6.10 the disappearance or appearance of the switching time occurs by a fold (or saddle-node) bifurcation of the zeros of f in which zeros coalesce. At the bifurcating zero, f has zero gradient and the transversality condition (6.22) is violated. Figures 6.9 and 6.10 are qualitative representations of switching time bifurcations; detailed simulation and experimental results on a single phase SVC circuit are presented in [14].

Switching time bifurcations are essentially bifurcations of the constraint condition determining the switching time and they differ in some respects from conventional bifurcations. For example, the eigenvalues of the Poincaré map Jacobian evaluated at the periodic orbit give no indication of either of the switching time bifurcations in Figures 6.9 and 6.10. In the case of the switching time bifurcations shown in Figure 6.10, the condition for the switching time bifurcation is the zero gradient of current at the new, earlier current zero and this condition has no relation to the Poincaré map Jacobian. (There is more subtlety in the case of the switching time bifurcations shown in Figure 6.9. At the switching time bifurcation $D\tau$ becomes infinite and it might be expected from formula (6.45) that this would imply that

DF_{s_2,s_1} and hence the Poincaré map Jacobian DP would have large eigenvalues outside the unit circle near the bifurcation. But this is false: the simplification (6.48) and formula (6.49) show that $D\tau$ has no effect on DP.)

Since the switching time is discontinuous at a switching time bifurcation and the Poincaré map depends on the switching time, the Poincaré map is also discontinuous at a switching time bifurcation [23, 25, 31] (see section 6.7.4). The switching time bifurcation can also be understood as the fixed point of the Poincaré map encountering the Poincaré map discontinuity. This aspect is emphasized by Wolf et al. [31].

6.7.2 Switching time bifurcations for transients

Switching time bifurcations also occur during transients and have interesting effects on the system dynamics as explained in the following subsections. This subsection and the remainder of section 6.7 explain these phenomena by summarizing mostly numerical results from [25] on the SVC example circuit specified in section 6.3. More detailed results and discussion may be found in [25]. All results assume that the thyristor firing pulses have a constant phase delay of 120° relative to the sinusoidal voltage source voltage crossings.

It is convenient to assume that a thyristor turns on at time zero. The initial state at time zero is given by $p = \mathbf{y}(0) = (V_c(0), I_s(0))^{\mathrm{T}}$ and is considered to be a parameter in order to study bifurcations of transients. The thyristor current function (6.19) or (6.72) is written $f(t, p)$.

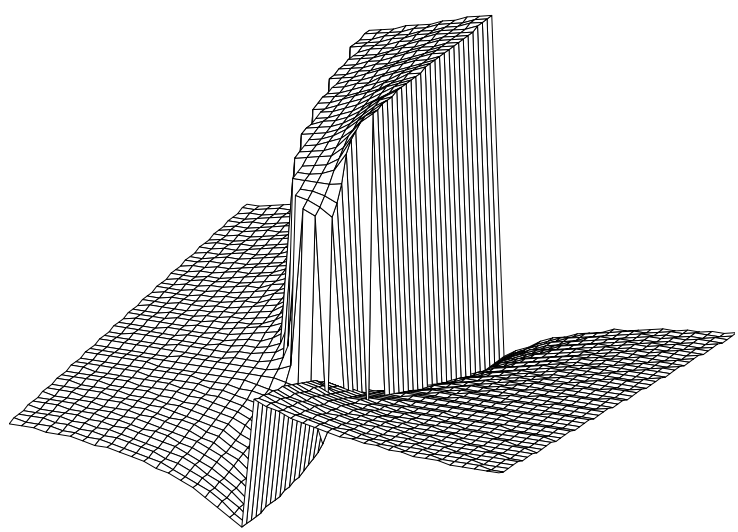

Figure 6.11: 3D plot of switch off time τ versus $p = (V_c(0), I_s(0))$.

The thyristor switching off time τ in the first half cycle is plotted as a function of the initial state $p = (V_c(0), I_s(0))^{\mathrm{T}}$ in Figure 6.11. Discontinuities of the switching time

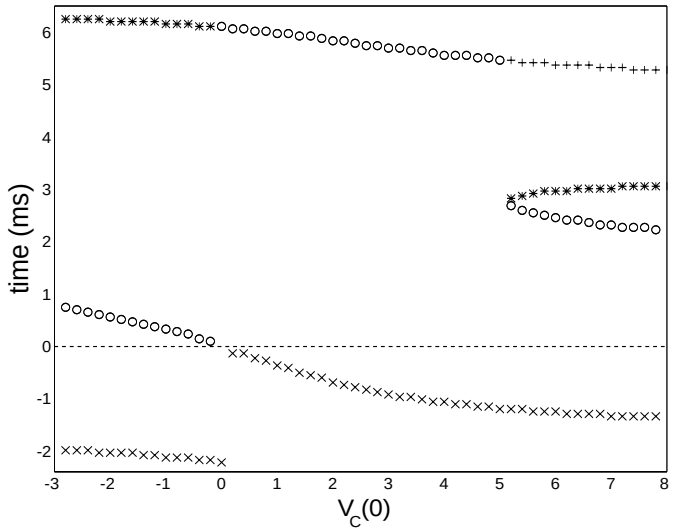

Figure 6.12: Roots of $f(t,p)$: $\circ$ = switch time τ, $*$ = root 2, $+$ = root 3, $\times$=root -1.

are apparent as sharp changes in the plot. These discontinuities can be understood by examining the roots of $f(t,p)$. Figure 6.12 shows a "slice" of Figure 6.11 obtained by plotting several roots of $f(t,p)$ versus the initial capacitor voltage $V_c(0)$ for a fixed initial source current $I_s(0) = 9$. The switching time τ is indicated by circles in the plot. As can be seen from Figure 6.12, a discontinuity in the switching time occurs near $V_c(0) = 5.1$ where the first and second roots of $f(t,p)$ coalesce and disappear in a fold bifurcation so that what was previously the third positive root becomes the first positive root and the switching time τ.

Graphs of f corresponding to a fold bifurcation as $V_c(0)$ varies and $I_s(0) = 4$ are shown in Figure 6.13. When $p = p_1 = (3.2, 4)^{\mathrm{T}}$, the transversality condition is satisfied at the thyristor switch off at $\tau(p_1)$ as shown in Figure 6.13a. There is a second root of f near $\tau(p_1)$ and a third root of f at a later time. When $p = p_* = (4.2, 4)^{\mathrm{T}}$ as in Figure 6.13b, f has zero gradient at the double root at $\tau(p_*)$ and the transversality condition is not satisfied. When p changes to a new value $p_2 = (5.2, 4)^{\mathrm{T}}$ near p_* as shown in Figure 6.13c, the previous first and second root have disappeared and the previous third root has suddenly become the first root.

6.7.3 Misfire onset as a transcritical bifurcation

A thyristor misfires at a switch on time if the thyristor voltage is negative when the gate turn on pulse arrives. Consider the thyristor firing at $t = 0$ (the analysis is similar for misfire at $t = T/2$). Just before the gate pulse arrives, at time $t = 0-$, the thyristor voltage is the capacitor voltage $V_c(0)$ (see Figure 6.1). From the system equations (6.2), $V_c(0)$ is the gradient of the thyristor current at $t = 0+$ or, equivalently, $\frac{\partial f}{\partial t}(0,p)$, the gradient of f at zero. Misfiring is described in the sequence of diagrams

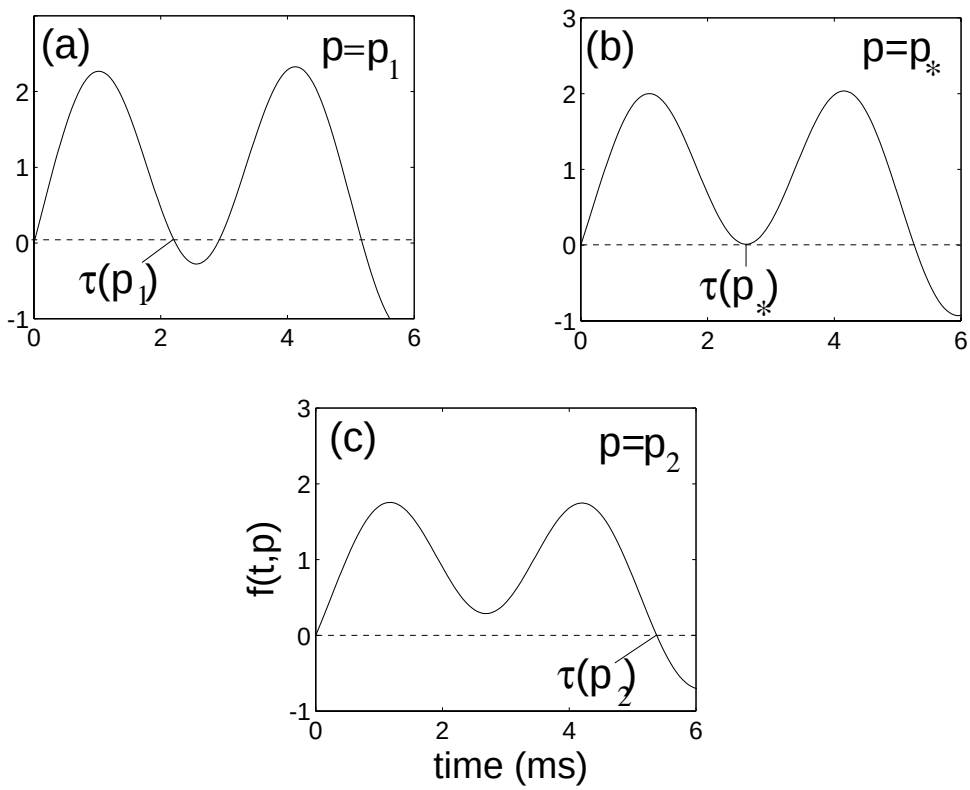

Figure 6.13: $f(t,p)$ versus t showing fold bifurcation

in Figure 6.14 which are plots of $f(t,p)$ versus t as $V_c(0)$ varies and $I_s(0) = 4$. In Figure 6.14a, $V_c(0) = 1$, the circuit is operating normally, and the gradient of f at zero is positive. In Figure 6.14b, $V_c(0) = 0$ and the gradient of f at zero has decreased to zero and this is the onset of misfire. In Figure 6.14c, $V_c(0) = -1$ and the thyristor will misfire since the gradient of f at zero is negative. If we define root –1 to be the first negative root of $f(t,p) = 0$, then root –1 increases through the root at zero and becomes relabeled as the first root when it becomes positive. The onset of the misfire occurs when root –1 coalesces with the root at zero. Since the root at zero is fixed, this is a transcritical bifurcation of roots of f. Also note that when $I_s(0) = 9$, a transcritical bifurcation diagram is evident at the origin of Figure 6.12. (A transcritical bifurcation generically occurs in a conventional dynamical system when two equilibria coalesce under the condition that one of the equilibria is fixed in position by the structure of the system. The bifurcation diagram is similar to two intersecting lines and the equilibria exchange stability when they coalesce. See [7, 29] for a detailed description of transcritical bifurcation.)

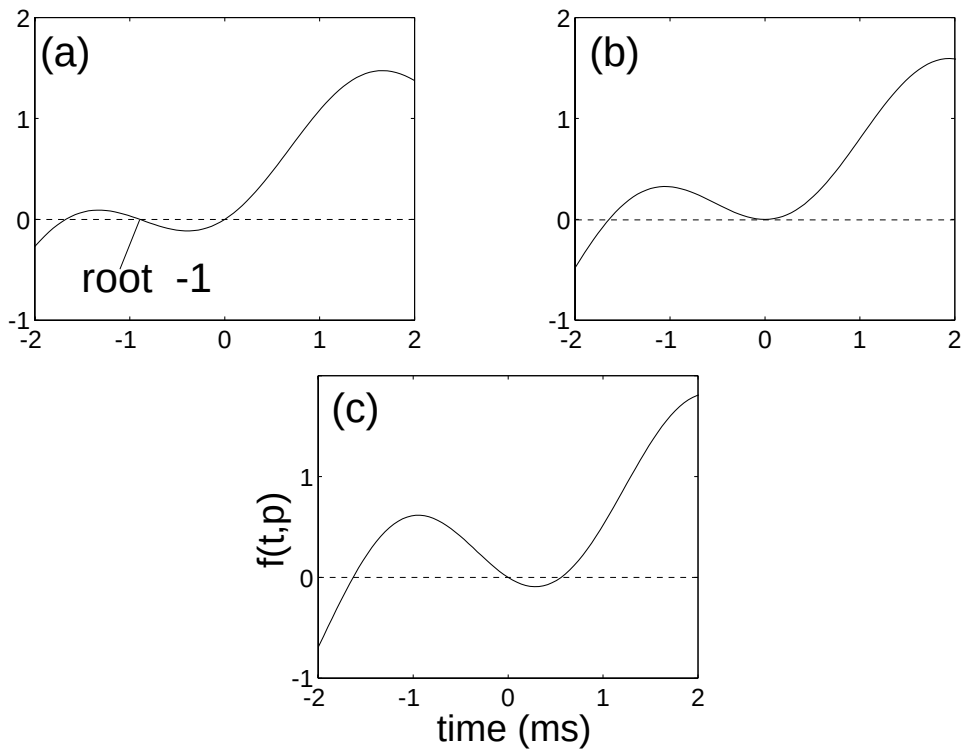

Figure 6.14: $f(t, p)$ versus t showing transcritical bifurcation

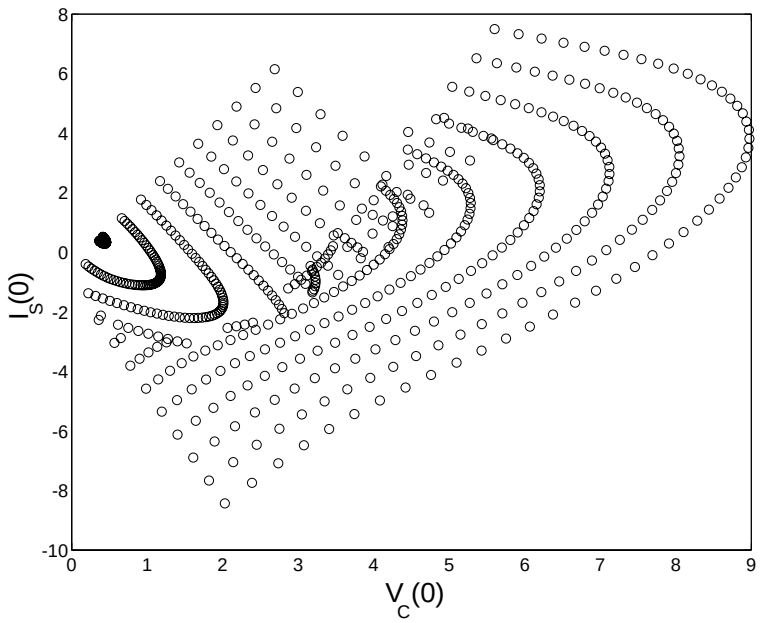

Figure 6.15: Poincaré map of semicircular disk

6.7.4 Noninvertibility and discontinuity of the Poincaré map

This section discusses how irreversibility of trajectories and switching time bifurcations can make the Poincaré map P respectively noninvertible and discontinuous.

Trajectories in thyristor circuits are sometimes reversible. Suppose that the thyristor is off and we wish to integrate the trajectory backwards in time. Regard the previous switch off time τ as a variable to be solved for. A constraint on τ can be found by requiring that integrating the on system backwards in time from time τ yields a current zero at the time of a firing pulse at which the thyristor turned on. If we can solve this constraint for τ (and also confirm that there was no misfire at the turn on), then a solution integrating the trajectory backwards in time until the previous switch on has been found. The problem is that the solution for τ need not be unique; there can be two distinct trajectories leading to the same state. A consequence of this irreversibility is that the Poincaré map is sometimes not invertible. This can be seen in the SVC example circuit by computing the Poincaré map for a segment of a semicircular disk of initial conditions and observing the overlapping portion of Figure 6.15.

The switching time bifurcations of section 6.7.2 cause the switching times in some transients to vary discontinuously as the initial condition is varied. That is, a switching time bifurcation can cause two initially nearby trajectories to separate greatly because a portion of one trajectory occurs in a circuit with a thyristor on while the same portion of the second trajectory occurs in a circuit with a thyristor off. Thus the switching time bifurcations cause discontinuities of the Poincaré map. If the initial condition

$\mathbf{y}(0)$ is such that a switching time bifurcation occurs at one of the switching times in the period, then P is discontinuous at $\mathbf{y}(0)$ [23, 25, 31]. We write Θ for the set of discontinuities of P. As shown in section 6.5 and proved in [5], P is smooth away from Θ. Wolf et al. [31] show interesting graphs of the Poincaré map discontinuities.

6.7.5 Multiple attractors and their basin boundaries

Numerical experiments for the SVC example circuit [23, 25] show that there are two asymptotically stable fixed points $\mathbf{y}_1$ and $\mathbf{y}_2$ of the Poincaré map; these correspond to two asymptotically stable periodic orbits of the circuit. This occurrence of multiple attractors can be surprising (in contrast, the corresponding diode circuits with suitable resistive damping containing diodes, voltage sources of period T, resistors, capacitors and inductors have unique attractors that are globally asymptotically stable).

A steady state (periodic orbit or fixed point) may be asymptotically stable, but a large disturbance may cause stability to be lost. The set of initial states which return to the steady state is called the basin of attraction of the steady state. (Think of a marble rolling in a bowl: the basin of attraction of the stable point at the bottom of the bowl is the inside of the bowl. Disturbances which perturb the state inside the bowl will decay as the marble eventually returns to bottom of the bowl. Larger disturbances will cause the marble to leave the bowl and roll away elsewhere. The boundary of the basin of attraction is the edge of the bowl.) The basin of attraction of a steady state is used to quantify the robustness to perturbations of that steady state. One way to describe the basins of attraction is to instead describe the boundaries of these basins.

In smooth dynamical systems, the essential mechanism which separates nearby trajectories so that they can tend to attractors in different basins is the saddle type behavior of unstable fixed points or periodic orbits in the basin boundary. The SVC circuit example has a basin boundary ∂B separating the basins of attraction of the two fixed points $\mathbf{y}_1$ and $\mathbf{y}_2$. However, there are no unstable fixed points in ∂B. ∂B interacts with the set of Poincaré map discontinuities Θ and the essential mechanism separating nearby trajectories to tend to attractors in different basins is the switching time bifurcations associated with Θ.

This is supported by numerical results for a portion of ∂B [26]: Figure 6.16a shows the fine structure of the Poincaré map discontinuities Θ. Θ is composed of 3 curves C_1, C_2, C_3. Initial conditions on C_1 yield switching time bifurcations in the first half cycle as shown in the corresponding inset of Figure 6.16(a) (the inset shows the qualitative form of thyristor current $I_r(t)$ for initial conditions on C_1 and $*$ indicates a switching time bifurcation). C_2 and C_3 correspond to switching time bifurcations in the second half cycle as shown in the corresponding insets of Figure 6.16a.

Figure 6.16b shows how the basin boundary ∂B intersects with Θ. The points in $\partial B \cap \Theta$ are initial conditions on the basin boundary which encounter a switching time bifurcation during the next cycle. The discontinuity in P caused by switching time bifurcation is the mechanism by which nearby initial conditions on either side of ∂B tend to different fixed points under iterations of P. Numerical results show that the points in ∂B not in Θ eventually map to $\partial B \cap \Theta$. That is, the basin boundary ∂B consists of initial conditions which are either on Θ or eventually map to Θ. However,

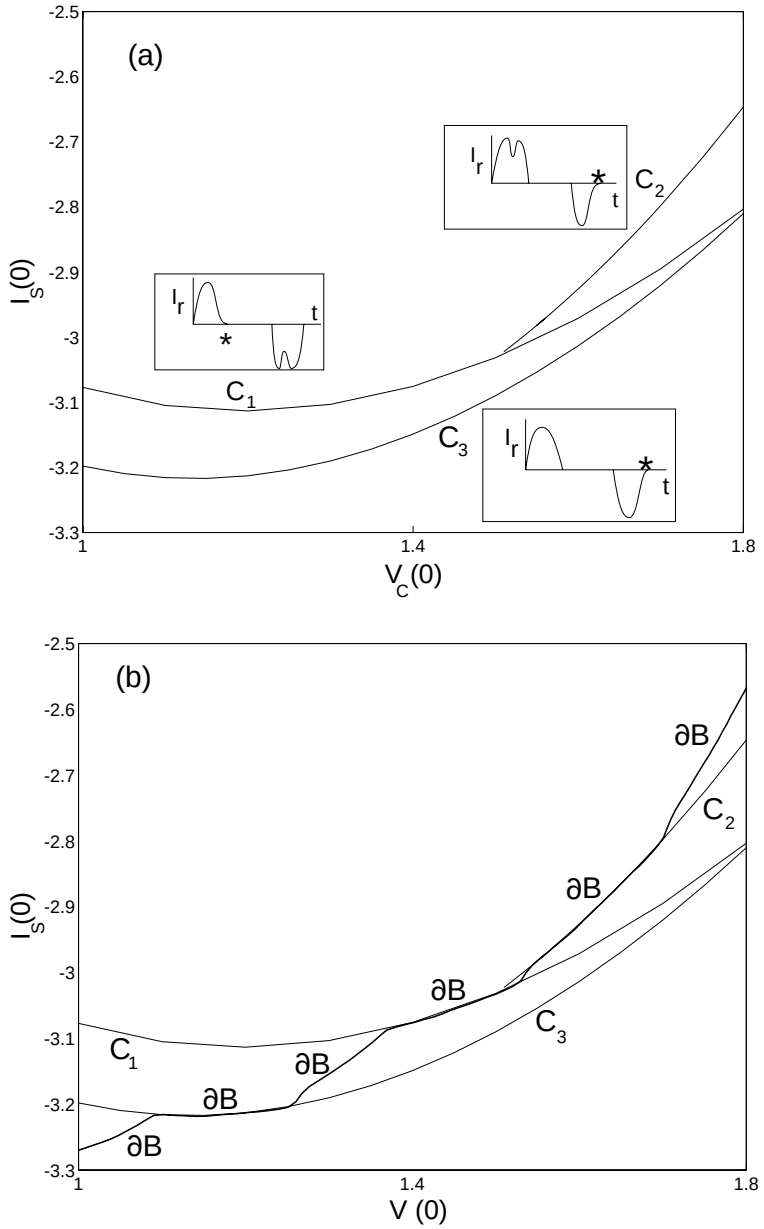

Figure 6.16: (a) Detail of Poincaré map discontinuities Θ. (b) Detail of basin boundary ∂B and Θ.

there are also many initial conditions in Θ but not in ∂B whose forward trajectories encounter switching time bifurcations.

The intricate and nonconventional structure of the basin boundary ∂B shows the great influence of switching time bifurcations and the thyristor switching rules on the system dynamics.

6.8 Diode circuits

This section considers circuits with ideal diodes. The analysis is useful in applications such as diode rectifier circuits and can be adapted to analyze circuits containing diodes and other switching elements, such as DC-DC convertors in a discontinuous mode of operation. The dynamics of diode circuits are generally simpler than the dynamics of thyristor circuits. Instead of describing the dynamics of diode circuits from scratch, it is convenient to describe the dynamics of diode circuits by comparing them to the dynamics of thyristor circuits.

6.8.1 Transversality and Poincaré map Jacobian formula

Diode switch off is the same as thyristor switch off and can be analyzed as described earlier in the chapter. Diode switch on occurs when diode voltage becomes positive and is analogous or dual to diode switch off. More precisely, diode switch on occurs at the first zero of diode voltage which is after the diode switch off. Similarly to section 6.5.1, the switch on is transversal if the gradient of the diode voltage is positive (taking the limit from below) at the switching on time.

Similarly to the case of diode or thyristor switch off in section 6.5.3, it is shown in [5] that at a transversal diode switch on, the map advancing the state over a time interval containing only this switch on is smooth and that its derivative is computed using formula (6.38). It follows by assembling the Jacobian as in section 6.5.3 that, if all the diode switchings in a cycle are transversal, the Poincaré map is smooth and its Jacobian is calculated by a formula such as (6.53). Formula (6.53) applies to the case of 4 diode switchings per cycle and the number of terms should be changed for other cases. For example [5], a symmetrical 3 phase diode bridge circuit in steady state Mode 1 operation with AC line impedance represented has Poincaré map Jacobian

$$DP = \left(e^{A_2(T/6-\mu)} R e^{A_3 \mu} Q\right)^6 \tag{6.73}$$

where A_2 corresponds to the circuit with two diodes conducting, A_3 corresponds to the commutating circuit with three diodes conducting, and μ is the commutation time. In this case, the symmetry of the circuit and the six time intervals containing noncommutating and commutating circuits gives an expression to the sixth power in (6.73).

6.8.2 Poincaré map Jacobian for the DC-DC buck-boost convertor in discontinuous mode

To illustrate the effect of the diode switching in the DC-DC buck-boost convertor we compute the Poincaré map Jacobian. Our notation follows that of Chapter 2. For simplicity, the switch is assumed to be switched once on and once off at fixed times in the cycle. Suppose the switch turns on at time 0 and that the Poincaré map sample time is chosen to be 0+. Then, as explained in detail in chapter 2, the cycle consists of an interval of duration $\delta_1 T$ with the switch on with state $\mathbf{x} = \begin{pmatrix} i \\ v \end{pmatrix}$ and matrix

$$A_1 = \begin{pmatrix} -R_l/L & 0 \\ 0 & -1/RC \end{pmatrix} \tag{6.74}$$

followed by an interval of duration $\delta_2 T$ with the switch off with state $\mathbf{x} = \begin{pmatrix} i \\ v \end{pmatrix}$ and matrix

$$A_2 = \begin{pmatrix} -R_l/L & 1/L \\ -1/C & -1/RC \end{pmatrix} \tag{6.75}$$

followed by an interval of duration $\delta_3 T$ with the diode off with state $\mathbf{y} = v$ and matrix

$$A_3 = -1/RC \tag{6.76}$$

It is necessary to correctly model the change in state space dimension when the diode switches off in order to obtain correct stability results. At the diode switch off, the matrix projecting the two dimensional state to the one dimensional state is

$$R = \begin{pmatrix} 0 & 1 \end{pmatrix} \tag{6.77}$$

At the switch on, the matrix augmenting the state space dimension from one to two is

$$Q = \begin{pmatrix} 0 \\ 1 \end{pmatrix} \tag{6.78}$$

The state is unchanged in dimension and continuous at the switch turn off.

Computing the Poincaré map Jacobian formula gives

$$\begin{aligned} DP &= Qe^{A_3\delta_3 T} R e^{A_2\delta_2 T} e^{A_1\delta_1 T} && (6.79) \\ &= \begin{pmatrix} 0 \\ 1 \end{pmatrix} e^{-\delta_3 T/RC} \begin{pmatrix} 0 & 1 \end{pmatrix} e^{A_2\delta_2 T} e^{A_1\delta_1 T} && (6.80) \\ &= \begin{pmatrix} 0 & 0 \\ 0 & e^{-\delta_3 T/RC} \end{pmatrix} e^{A_2\delta_2 T} e^{A_1\delta_1 T} && (6.81) \end{aligned}$$

It is clear that DP has a zero eigenvalue and that $DP \begin{pmatrix} \delta i \\ \delta v \end{pmatrix}$ has first component zero for any linearized perturbation $\begin{pmatrix} \delta i \\ \delta v \end{pmatrix}$. This means that the circuit damps any initial perturbation δi in inductor current to zero at the end of the cycle; this is clearly

correct since the inductor current is constrained to be zero at the end of the cycle because of the diode being off.

Neglecting the change in state space dimension by assuming that, when the diode is not conducting, $\mathbf{x} = \begin{pmatrix} i \\ v \end{pmatrix}$ and

$$A_3 = \begin{pmatrix} 0 & 0 \\ 0 & -1/RC \end{pmatrix} \tag{6.82}$$

would yield

$$\begin{aligned} DP &= e^{A_3\delta_3 T} e^{A_2\delta_2 T} e^{A_1\delta_1 T} && (6.83) \\ &= \begin{pmatrix} 1 & 0 \\ 0 & e^{-\delta_3 T/RC} \end{pmatrix} e^{A_2\delta_2 T} e^{A_1\delta_1 T} && (6.84) \end{aligned}$$

which is wrong. In particular, (6.84) would generally imply a nonzero current perturbation at the end of a cycle.

Instead of choosing the Poincaré map sample time at 0+, which is done above so that it can be more directly compared with the wrong calculation (6.84), it is usually more convenient to choose the Poincaré map sample time at 0−. Then the Poincaré map Jacobian becomes the scalar

$$DP = e^{A_3\delta_3 T} R e^{A_2\delta_2 T} e^{A_1\delta_1 T} Q \tag{6.85}$$

For example, the Poincaré map sample time at 0− is used in chapter 5.5.2.

6.8.3 Poincaré map continuity and switching time bifurcations

Consider a circuit of ideal diodes, time dependent sources and resistors, inductors and capacitors. It can be shown [5] using incremental energy methods that the Poincaré map is continuous. The diode switch offs decrease incremental energy and provide switching damping to the circuit as in the case of thyristor switch offs. (Diode switch ons also decrease incremental energy, but this is a second order effect.)

The Poincaré map is not differentiable when one of the switchings is not transversal (the Jacobian has a discontinuity) and a switching time bifurcation can then occur. However, the typical consequences of the switching time bifurcation differ from those in thyristor circuits. In diode circuits a new diode switch off generally appears or disappears together with a closely following diode switch on [5]. The consequence of the switching time bifurcation is then a mode change in the circuit in which a short time interval with a particular pattern of diode conduction appears or disappears.

This behavior occurs in the simple diode circuit shown in Figure 6.17 when the circuit resistance is positive. When the constant bias p of the voltage source lies in the interval $(-1, 0)$, there is a unique and asymptotically stable periodic orbit in which the diode switches twice per cycle. In this mode, the Poincaré map at the periodic orbit with initial time when the diode is off simply maps zero incremental current to zero incremental current and the Jacobian of the Poincaré map is zero. That is, a small perturbation in one cycle vanishes before the next cycle.

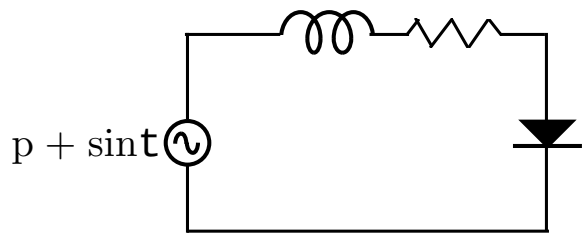

Figure 6.17: Simple diode circuit showing mode changes.

If p increases through 0, the periodic orbit persists and remains asymptotically stable, but the diode never turns off. The stability of the periodic orbit is now governed by the resistor so that the Jacobian of the Poincaré map changes discontinuously when p increases through zero. If p decreases through -1, the periodic orbit becomes a constant zero current and the diode never turns on. In both these switching time bifurcations, the two switching times coalesce and disappear. The effect of the switching time bifurcations is a mode change in the circuit and asymptotic stability is not lost. Note, however, that in the extreme case of zero circuit resistance, the periodic orbit, although stable for $p \leq 0$, disappears for $p > 0$ and the circuit trajectory becomes unbounded.

6.9 Firing angle control

Practical high power thyristor circuits control the firing angle both to regulate performance with closed loop controls and to synchronize the firing with the AC waveform. Since these important effects are omitted from the previous analysis in the chapter, this section briefly introduces an example of the appropriate modifications to the Jacobian formula for the SVC example circuit. Control and synchronization both have important effects on the circuit stability [13].

We proceed by modifying the analysis from section 6.5.3 to account for changes in the thyristor firing angle. Section 6.5.3 considered a time interval $[s_2, s_3]$ including a thyristor switch on at time ϕ and no other switchings. F_{s_3,s_2} is the flow which maps the initial state $\mathbf{y}(s_2)$ at s_2 to the final state $\mathbf{x}(s_3)$ at s_3 and section 6.5.3 computed that

$$DF_{s_3,s_2} = DG_{s_3,s_2} + \frac{\partial G_{s_3,s_2}}{\partial \phi} D\phi \tag{6.86}$$

where G_{s_3,s_2} is given by (6.36). Differentiating (6.36) yields

$$\begin{aligned} \frac{\partial G_{s_3,s_2}}{\partial \phi} &= e^{A_{\text{on}}(s_3-\phi)}(QR - I)(A_{\text{on}}\mathbf{x}(\phi) + B_{\text{on}}u(\phi)) \\ &= e^{A_{\text{on}}(s_3-\phi)}c^{\text{T}}c\,\dot{\mathbf{x}}(\phi+) \end{aligned} \tag{6.87}$$

where $c = (\,1 \quad 0 \quad 0\,)$. (An interesting alternate expression is

$$\frac{\partial G_{s_3,s_2}}{\partial \phi} = e^{A_{\text{on}}(s_3-\phi)}(Q\dot{\mathbf{y}}(\phi-) - \dot{\mathbf{x}}(\phi+)) \tag{6.88}$$

but this is not necessary here.) Now (6.86) becomes

$$DF_{s_3,s_2} = e^{A_{\text{on}}(s_3-\phi)} Q e^{A_{\text{off}}(\phi-s_2)} + e^{A_{\text{on}}(s_3-\phi)} c^{\mathrm{T}} c\, \dot{\mathbf{x}}(\phi+) D\phi \tag{6.89}$$

and the effect of the controlled switch on is captured in the second term of (6.89).

It remains to compute $D\phi$ according to the control or synchronization represented. Obtaining a formula for $D\phi$ can be difficult particularly if the control depends on a filtered version of the past system states. However, some cases are tractable [13] and here we illustrate the calculation of $D\phi$ for current synchronization. The row vector $D\phi$ is the gradient of the turn on time ϕ with respect to $\mathbf{y}(s_2)$.

Synchronizing the firing with respect to the zeros of the line current I_s is modeled by

$$\phi = \zeta + (\pi - \sigma_{req})/2 \tag{6.90}$$

where ζ is the time of the current zero and σ_{req} is the required thyristor conduction time. ζ satisfies the constraint

$$0 = I_s(\zeta) = ny(\zeta) = nG_{\zeta,s_2}\left(\mathbf{y}(s_2), \zeta(\mathbf{y}(s_2))\right) \tag{6.91}$$

where $n = (0, 1, 0)$. ζ is assumed to occur when both thyristors are off.

Differentiating the constraint (6.91) yields

$$0 = nDG_{\zeta,s_2} + n\frac{\partial G_{\zeta,s_2}}{\partial \zeta} D\zeta \tag{6.92}$$

Now differentiation of (6.90) and solving (6.92) yields

$$D\phi = D\zeta = \frac{-nDG_{\zeta,s_2}}{n\frac{\partial G_{\zeta,s_2}}{\partial \zeta}} = \frac{-ne^{A_{\text{off}}(\zeta-s_2)}}{n\dot{\mathbf{y}}(\zeta)} \tag{6.93}$$

Bibliography

[1] L.O. Chua, M. Hasler, J. Neirynck, P. Verburgh, Dynamics of a piecewise-linear resonant circuit, *IEEE Trans. Circuits and Systems*, vol. 29, no. 8, August 1982, pp. 535-547.

[2] E.A. Coddington, N. Levinson, *Theory of ordinary differential equations*, Chapter 13, section 2, reprint, Krieger Publishing Company, Malabar FL USA, 1984.

[3] I. Dobson, S.G. Jalali, Surprising simplification of the Jacobian of a switching circuit, *IEEE International Symposium on Circuits and Systems*, Chicago, IL, May 1993, pp. 2652-2655.

[4] I. Dobson, S.G. Jalali, R. Rajaraman, Damping and resonance in a high power switching circuit, in *Systems and control theory for power systems* (eds. J.H. Chow, P.V. Kokotovic, R.J. Thomas), IMA volume 64 in mathematics and its applications, Springer Verlag, New York, pp. 137-156, 1995.

[5] I. Dobson, Stability of ideal thyristor and diode switching circuits, *IEEE Trans. Circuits and Systems, Part 1*, vol. 42, no. 9, September 1995, pp. 517-529.

[6] M. Grötzbach, R. von Lutz, Unified modelling of rectifier-controlled DC-power supplies, *IEEE Trans. Power Electronics*, vol. 1, no. 2, April 1986, pp. 90-100.

[7] J. Guckenheimer, P. Holmes, *Nonlinear oscillations, dynamical systems and bifurcations of vector fields*, Springer-Verlag, NY, 1986.

[8] L. Gyugyi, Power electronics in electric utilities: static var compensators, *Proceedings IEEE*, vol. 76, no. 4, April 1988, pp. 483-494.

[9] J.K. Hale, *Oscillations in nonlinear systems*, McGraw Hill, NY, 1963.

[10] J.G. Kassakian, M.F. Schlecht, G.C. Verghese, *Principles of Power Electronics*, Addison-Wesley, Reading MA, 1992.

[11] J.P. Louis, Non-linear and linearized models for control systems including static convertors, Proceedings of the Third Intl. Federation on Automatic Control Symposium on Control in power electronics and electrical drives, Lausanne, Switzerland, September 1983, pp. 9-16.

[12] S.G. Jalali, I. Dobson, R.H. Lasseter, Instabilities due to bifurcation of switching times in a thyristor controlled reactor, *Power Electronics Specialists Conference*, Toledo, Spain, July 1992, pp. 546-552.

[13] S.G. Jalali, R.H. Lasseter, I. Dobson, Dynamic response of a thyristor controlled switched capacitor, *IEEE Transactions on Power Delivery*, vol. 9, no. 3, July 1994, pp.1609-1615.

[14] S.G. Jalali, I. Dobson, R.H. Lasseter, G. Venkataramanan, Switching time bifurcations in a thyristor controlled reactor, *IEEE Transactions on Circuits and Systems, Part 1*, vol. 43, no. 3, March 1996, pp. 209-218.

[15] S.G. Jalali, Harmonics and instabilities in thyristor based switching circuits, Ph.D. Thesis, University of Wisconsin–Madison, 1993.

[16] P. Kundur, *Power system control and stability*, McGraw Hill, New York, 1994

[17] R. von Lutz, M. Grötzbach, Straightforward discrete modelling for power convertor systems, *Power Electronics Specialists Conference*, Toulouse, France, June 1985, pp. 761-770.

[18] P. Mattavelli, A.M. Stankovic, G.C. Verghese, SSR analysis with dynamic phasor model of thyristor-controlled series capacitor *IEEE Transactions on Power Systems*, vol. 14, no. 1, February 1999, pp. 200-208.

[19] T.J.E. Miller, ed., *Reactive power control in electric systems*, Wiley NY, 1982.

[20] H.A. Othman, L. Ängquist, Analytical modeling of thyristor-controlled series capacitors for SSR studies, *IEEE Transactions on Power Systems*, vol. 11, no. 1, February 1996, pp. 119-127.

[21] B.K. Perkins, M.R. Iravani, Dynamic modeling of a TCSC with application to SSR analysis, *IEEE Transactions on Power Systems*, vol. 12, no. 4, November 1997, pp. 1619-1625.

[22] B.K. Perkins, M.R. Iravani, Dynamic modeling of high power static switching circuits in the dq-frame, *IEEE Transactions on Power Systems*, vol. 14, no. 2, May 1999, pp. 678-684.

[23] R. Rajaraman, I. Dobson, S.G. Jalali, Nonlinear dynamics and switching time bifurcations of a thyristor controlled reactor, *IEEE International Symposium on Circuits and Systems*, Chicago, IL, May 1993, pp. 2180-2183.

[24] R.Rajaraman, *Damping of subsynchronous resonance and nonlinear dynamics in thyristor switching circuits*, PhD thesis, Univ. of Wisconsin-Madison, 1996.

[25] R. Rajaraman, I. Dobson, S. Jalali, Nonlinear dynamics and switching time bifurcations of a thyristor controlled reactor circuit, *IEEE Transactions on Circuits and Systems, Part 1*, vol. 43, no. 12, December 1996, pp. 1001-1006.

[26] R. Rajaraman, I. Dobson, Damping and incremental energy in thyristor switching circuits, *IEEE International Symposium on Circuits and Systems*, Seattle, Washington, May 1995, pp. 291-294.

[27] R. Rajaraman, I. Dobson, R.H. Lasseter, Y. Shern, Computing the damping of subsynchronous oscillations due to a thyristor controlled series capacitor, *IEEE Transactions on Power Delivery*, vol. 11, no. 2, April 1996, pp. 1120–1127.

[28] S.R. Sanders, G.C. Verghese, Lyapunov-based control for switched power converters, *IEEE Trans. Power Electronics*, vol. 7, no. 1, Jan. 1992, pp. 17-24.

[29] S. Strogatz, Nonlinear dynamics and chaos : with applications in physics, biology, chemistry, and engineering, Addison-Wesley, Reading MA, 1994.

[30] G.C. Verghese, M.E. Elbuluk, J.G. Kassakian, A general approach to sampled-data modeling for power electronic circuits, *IEEE Trans. on Power Electronics*, vol. 1, no. 2, April 1986, pp. 76-89.

[31] D.M. Wolf, M. Varghese, S.R. Sanders, Bifurcation of power electronic circuits, Section 5, *Journal of the Franklin Institute- Engineering and Applied Mathematics*, vol. 331B, no. 6, November 1994, pp. 957-999.